AD NUMBER

AD818424

NEW LIMITATION CHANGE

TO

Approved for public release, distribution unlimited

FROM

Distribution authorized to U.S. Gov't. agencies and their contractors; Administrative/Operational Use; JUL 1967. Other requests shall be referred to Air Force Weapons Lab., Kirtland AFB, NM.

AUTHORITY

AFWL ltr 30 Nov 1971

EXPONENTIALLY DECAYING PRESSURE PULSE MOVING WITH SUPERSEISMIC VELOCITY ON THE SURFACE OF A HALF SPACE OF GRANULAR MATERIAL

Hans H. Bleich Alva Matthews

Paul Weidlinger, Consulting Engineer
New York, New York 10017

Contract AF 29(601)-7082

TECHNICAL REPORT NO. AFWL-TR-67-21

July 1967

AIR FORCE WEAPONS LABORATORY
Research and Technology Division
Air Force Systems Command
Kirtland Air Force Base
New Mexico

AFWL-TR-67-21

Research and Technology Division
AIR FORCE WEAPONS LABORATORY
Air Force Systems Command
Kirtland Air Force Base
New Mexico

EXPONENTIALLY DECAYING PRESSURE PULSE MOVING WITH SUPERSEISMIC VELOCITY ON THE SURFACE OF A HALF SPACE OF GRANULAR MATERIAL

Hans H. Bleich Alva Matthews

Paul Weidlinger, Consulting Engineer
New York, New York 10017
Contract AF 29(601)-7082

TECHNICAL REPORT NO. AFWL-TR-67-21

FOREWORD

This report was prepared by Paul Weidlinger, Consulting Engineer, New York, New York, under Contract AF 29(601)-7082. The research was performed under Program Element 7.60.06.01.D, Project 5710, Subtask 13.144, and was funded by the Defense Atomic Support Agency (DASA).

Inclusive dates of research were May 1966 to May 1967. The report was submitted 12 June 1967 by the Air Force Weapons Laboratory Project Officer, Lt H. F. Cooper, Jr. (WLDC).

This technical report has been reviewed and is approved.

H. F. COOPER, JR.
Lt, USAF
Project Officer

ALLEN F. DILL
CDR, CEC, USNR
Chief, Civil Engineering Branch

GEORGE C. DARBY, JR.
Colonel, USAF
Chief, Development Division

ABSTRACT

(Distribution Limitation Statement No. 2)

An approximate solution is given for the effect of an exponentially decaying pressure pulse traveling with superseismic velocity on the surface of a half space. The material of the half space is an elastic-plastic model of a material having internal Coulomb friction. The yield condition selected may be suitable for a granular material. The effect of a step wave for this geometry and medium was treated previously. For that case, the peak pressures do not decrease with increase in depth, while such a decrease is obtained for a decaying surface load. It was the prime purpose of this investigation to determine the magnitude of this attenuation. The approximate solutions obtained are valid for a limited distance behind the wave front, and are tabulated for 11 different sets of parameters pertaining to the material and velocity. The tabulated results show that the peak pressures in the case of the decaying surface load do decrease with depth, but that the decrease is less than one might intuitively expect.

CONTENTS

LIST OF SYMBOLS

a_i , b_i , c_i	Coefficients of Taylor series expansion.
c_P , c_S , $\bar{c}$	Velocity of propagation of elastic P-waves, S-waves, and inelastic shock fronts, respectively.
f_i , g_i	Arbitrary functions of x or y.
$F = 0$	Yield condition, Eq. (1).
G	Shear modulus.
J_1 , J_2	Invariants, Eqs. (2) and (3).
$K = \frac{2(1+\nu)}{3(1-2\nu)} G$	Bulk modulus.
$M = \frac{V}{c_P}$, $M_S = \frac{V}{c_S}$	
n	Ratio defined by Eq. (8).
N_1 ,..., N_{10}	Functions defined by Eq. (77).
$p(x - Vt)$	Surface pressure.
p_o	Initial values of surface pressure.
t	Time.
u, v, $\dot{u}$, $\dot{v}$	Particle displacements and velocities in x and y directions, respectively.
$\dot{u}_N$, $\dot{u}_T$	Particle velocities normal and tangential, respectively to fronts of discontinuity.
V	Velocity of surface pressure.
x, y	Cartesian coordinates.
α	Material parameter related to angle of internal friction.
$\Delta\sigma$, $\Delta\dot{u}$, $\Delta\tau$	Increments of σ, $\dot{u}$, τ, etc. at a front.

ϵ_i	Strain rates.
$\xi = x - Vt$	Coordinate.
θ	Angle between direction of principal stress σ_1 and x-axis.
μ	Decay constant of surface pressure, Eqs. (46) and (115).
ν	Poisson's ratio.
ρ	Mass density of medium.
σ_i , τ	Normal and shear stresses, respectively.
σ_1 , σ_2 , σ_3	Principal stresses.
σ_N , τ_N , σ_T	Stresses, respectively in the plane, and perpendicular to the plane of a shock front.
φ	Position angle of element, Fig. 8.
φ_P , φ_S , $\bar{\varphi}$	Position angle of elastic P- and S- and inelastic shock fronts, respectively.
Φ, Ψ, $\bar{\Psi}$, $\bar{\bar{\Psi}}$	Potential functions.

SECTION I

INTRODUCTION

In a preceding report, Ref. [1]*), the effect of a step pressure, Fig. 1, progressing with superseismic velocity V on the surface of a half-space has been studied for the limiting case $k \to 0$, for an elastic-plastic material subject to the yield condition

$$F = \left|\sqrt{J_2}\right| + \alpha J_1 - k \cong \left|\sqrt{J_2}\right| + \alpha J_1 = 0 \qquad (1)$$

where J_1 and J_2 are the invariants

$$J_1 = \sigma_{ii} \qquad (2)$$

$$J_2 = \frac{1}{2} s_{ij} s_{ij} \qquad (3)$$

while the coefficient α defines the internal friction of the material. The value α is subject to the limitations $0 \leq \alpha \leq \sqrt{\frac{1}{12}}$, Ref. [1].

The present paper will consider the more general problem of a decaying pressure signal $p(x - Vt)$, Fig. 2, moving also with superseismic velocity V. The problem to be studied here is, from a practical point of view, more realistic than the one treated in [1], but the case shown in Fig. 2 is also considerably more complex. The complexity is such that only an approximate solution will be derived which is valid for a limited distance from the wave front. The approximation to be employed suggests itself when considering the results of the analysis [1] for the step wave.

It was found in [1] that the response changes in character depending on the range in which the values of Poisson's ratio ν and of the material parameter α are situated, Fig. 3. The values α of practical interest lie between 0.1 and 0.2,

*) [1] Bleich, H.H., Matthews, A.T. and Wright, J.P., Step Load Moving with Superseismic Velocity on the Surface of a Half-Space of Granular Material, Tech. Rpt. AFWL-TR-65-59, Air Force Systems Command, Kirtland AFB, September 1965.

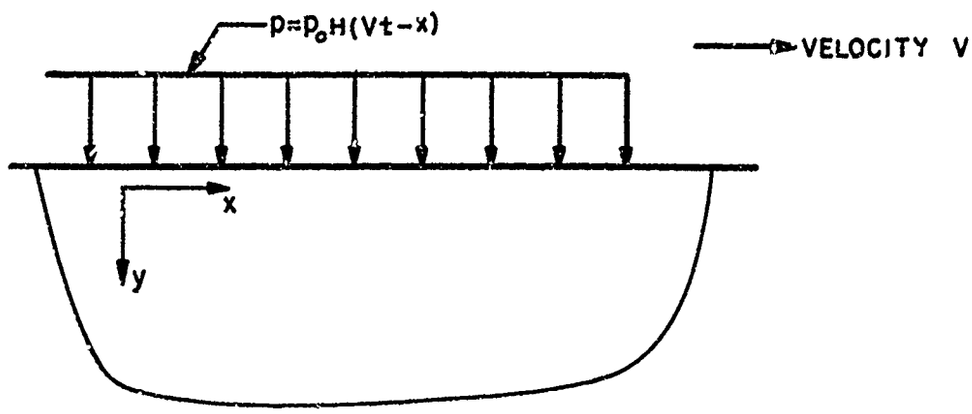

FIG. 1

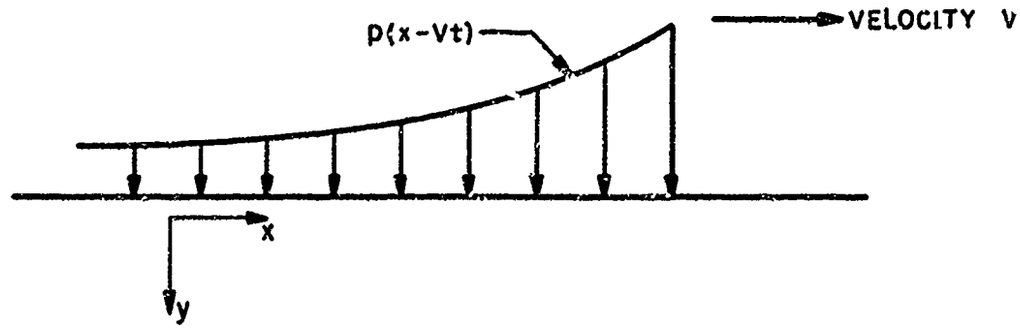

FIG. 2

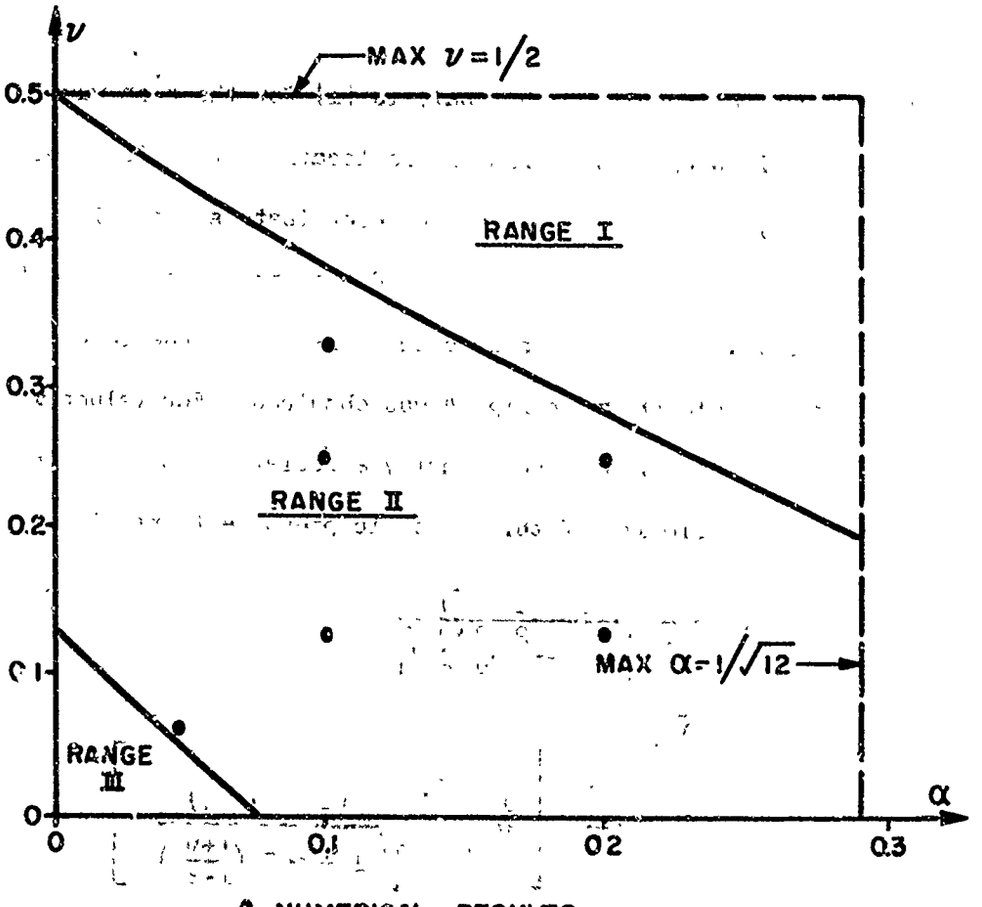

FIG. 3—PRINCIPAL RANGES

otherwise the value of the angle of internal friction becomes unreasonably small, or unreasonably large. For values of α limited by $0.10 < \alpha < 0.20$, Range III never applies, so that this range can be ignored, and only Ranges I and II will be studied further.

Range II

Consider first the result of the analysis [1] for the step wave for parameters ν and α in Range II. Defining the location of a field point by polar coordinates φ and r, where the origin of the coordinate system lies at, and moves with the front of the load, it was found that the stresses are functions of the angle φ only, i.e., for a step load there is no dependence on r. In Range II, the stress field shown in Fig. 4 was obtained. For values $\varphi < \bar{\varphi}$, all stresses vanish while a stress discontinuity associated with plastic deformations occurs at $\varphi = \bar{\varphi}$. The velocity of this "plasti essure front" is

$$c^2 = \frac{K}{\rho} \frac{(1 + 2\alpha\sqrt{3})^2}{\left[1 + 6\alpha^2 \left(\frac{1+\nu}{1-2\nu}\right)\right]} \tag{4}$$

which defines the angle $\bar{\varphi}$

$$\bar{\varphi} = \pi - \sin^{-1}\left[\frac{1}{V}\sqrt{\frac{K}{\rho}}\frac{(1 + 2\alpha\sqrt{3})}{\sqrt{1 + 6\alpha^2\left(\frac{1+\nu}{1-2\nu}\right)}}\right] \tag{5}$$

The stress discontinuity at the front is such that no discontinuity in shear parallel to the front occurs. Between $\bar{\varphi}$ and φ_S there is no change in stress at all, i.e., the material is not subjected to plastic deformations. At $\varphi = \varphi_S$ there is an elastic discontinuous change in shear, moving with the velocity of elastic shear waves

$$c_S^2 = \frac{G}{\rho} \tag{6}$$

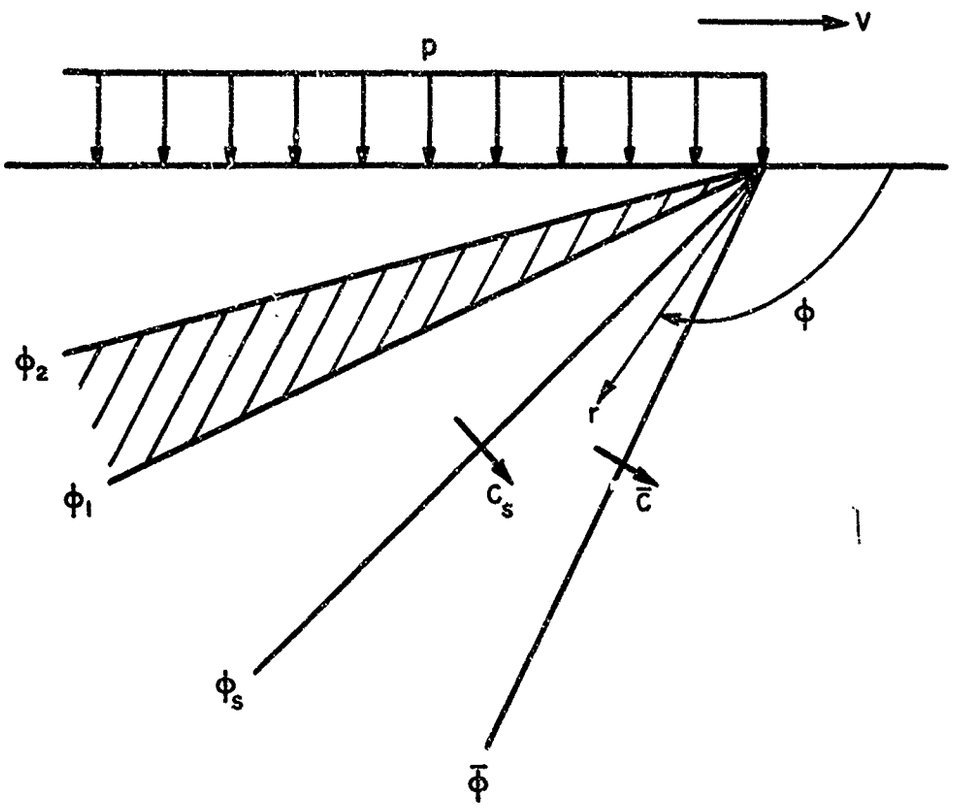

FIG. 4 CONFIGURATION IN RANGE II

which defines

$$\varphi_S = \pi - \sin^{-1}\left[\frac{1}{V}\sqrt{\frac{G}{\rho}}\right] \tag{7}$$

In Range IIb, which covers most of Range II, see Figs. 9b-e of [1], one finds that, from φ_S to a value φ_1 and again from φ_2 to the surface, the stresses are constant and no inelastic deformations occur. However, between φ_1 and φ_2 inelastic deformations do occur, and the stresses vary with φ. Details of the variation, and the values $\bar{\varphi}$, φ_S, φ_1 and φ_2 are given in Table I of Ref. [1]. (No plastic region φ_1 to φ_2 occurs in a small portion of Range II, called Range IIa in [1].)

As described above, plastic deformations occur therefore in at most two locations, at the plastic front $\bar{\varphi}$, and between φ_1 and φ_2. The prime purpose of the preceding description is to note, further, that the plastic changes in stress between φ_1 and φ_2 as shown in [1] are small compared to the change at the front $\bar{\varphi}$. This suggests that one could find an approximate solution that has a plastic front at $\bar{\varphi}$, but which satisfies everywhere else the differential equations for elastic changes in stress and strain. Formulating the problem in this fashion, one will find that the yield condition will be violated in some locations, if ν and α are in Range IIb. However, one might accept such a solution, if the degree of violation of the yield condition is not severe. The violation can be recognized by the excess of the ratio

$$n = \left|\frac{\sqrt{J_2}}{\alpha J_1}\right| \tag{8}$$

above unity. Figure 5 shows the violation of the yield condition for the results of such an approximate analysis for the case of the step wave for typical values of ν, α, and of the velocity ratio V/c_p. It is seen that the

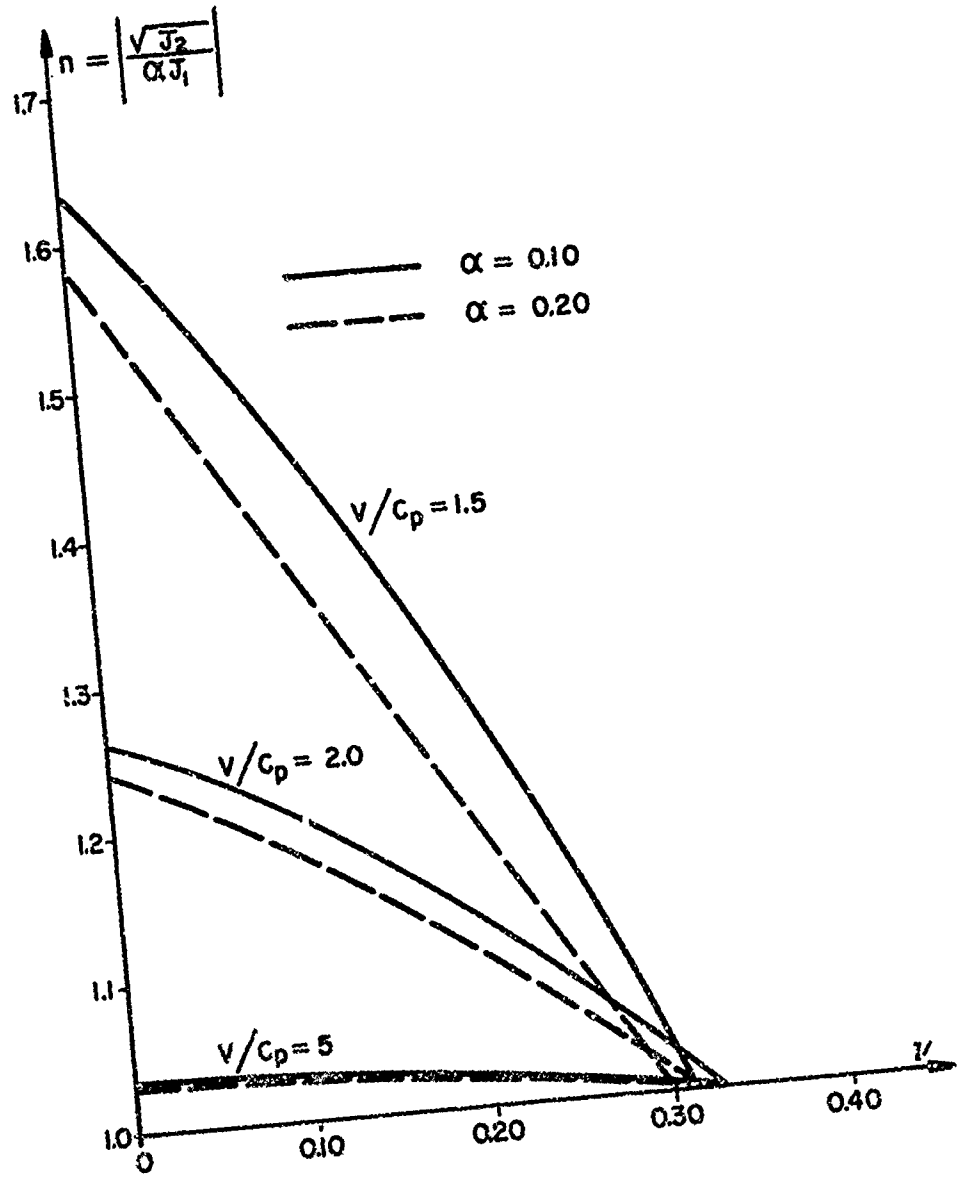
$n = \left|\frac{\sqrt{J_2}}{\alpha J_1}\right|$
1.7
1.6
1.5
1.4
1.3
1.2
1.1
1.0
α = 0.10
α = 0.20
V/Cp = 1.5
V/Cp = 2.0
V/Cp = 5
1/
0
0.10
0.20
0.30
0.40

FIG. 5

violations are very small for large values of V/c_p ; they may exceed 20% for $V/c_p < 2$. As a first approximation for engineering purposes one may accept violations up to 20%, i.e., $\left| \frac{\sqrt{J_2}}{\alpha J_1} \right| < 1.2$. This order of violation is considered acceptable here, because the prime purpose of the present analysis is to demonstrate the difference between the effect of a step wave, Fig. 1, and the effect of a decaying wave, Fig. 2. When results are obtained later, checks will be made to confirm the magnitude of the violation of the yield condition in various locations, so that the usefulness and the range of applicability of the approximate solution can be judged.

Range I

The difference in the results for the step wave in Ranges I and II lies in the fact that in Range I there is no plastic shock front, instead there is an elastic shock front moving with the velocity of P-waves

$$c_p^2 = \frac{2(1-\nu)G}{(1-2\nu)\rho} \tag{9}$$

The location of this front, Fig. 6, is defined by the angle

$$\varphi_p = \pi - \sin^{-1}\left[\frac{1}{V} \sqrt{\frac{2(1-\nu)G}{(1-2\nu)\rho}} \right] \tag{10}$$

Following this shock, the pattern is in principle the same as in Range II, and there is a division in Subranges Ia and Ib. In Subrange Ib, which covers only a minute portion of Range I, see Figs. 9b-e of Ref. [1], there is an S-front and a plastic region of very small extent from φ_1 to φ_2 , Fig. 6. In Subrange Ia, which covers most of Range I, there is an S-front, but no plastic region. In Subrange Ia the solution is entirely elastic so that the stress field without approximation can be found from Ref. [2]*). In Range Ib, the plastic effects occur

*) [2] Baron, M.L., Bleich, H.H. and Weidlinger, P., Theoretical Studies in Ground Shock Phenomena, SR-19, The MITRE Corporation, October 1960.

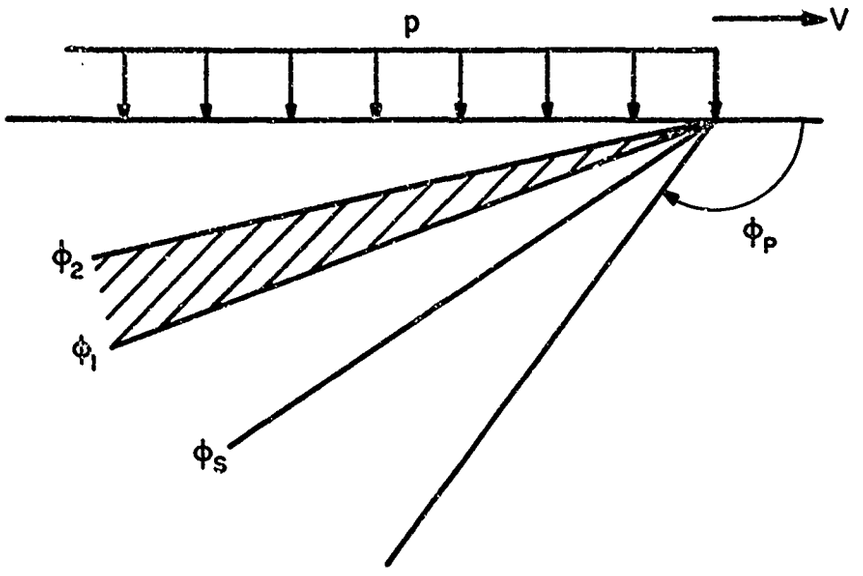

FIG.6 CONFIGURATION FOR RANGE I b

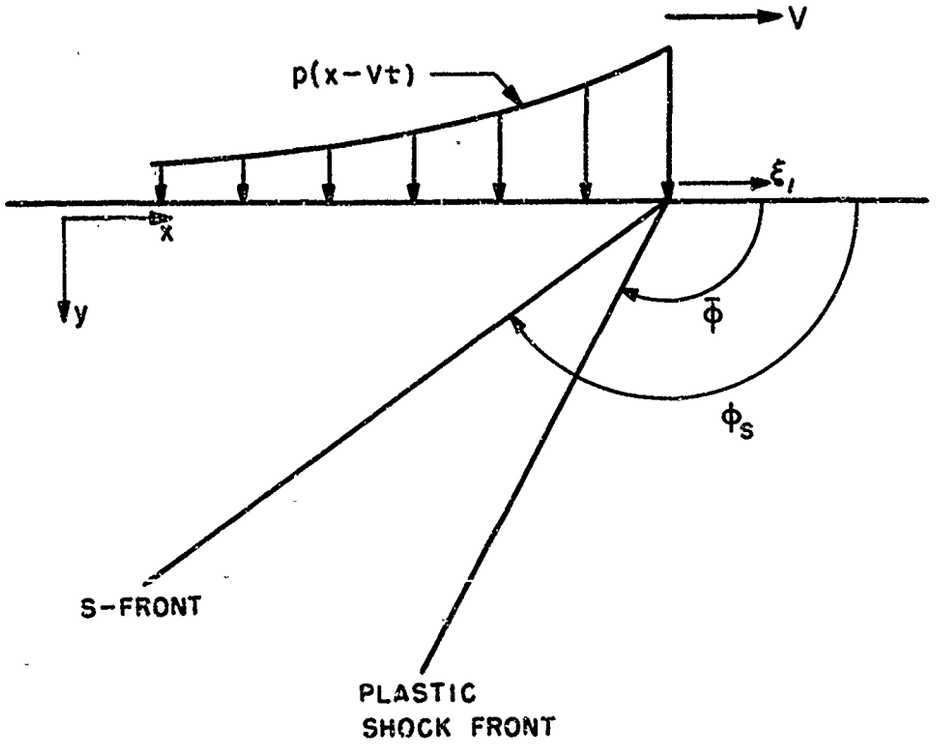

FIG.7 ASSUMED CONFIGURATION

only in a minute region φ_1 to φ_2 and are minor. If, similar to the above suggestion for Range II, this plastic region is ignored, the solution may be obtained, this time approximately, from Ref. [2]. There will therefore be no need to obtain a new approximate analysis for Range I at all.

SECTION II

FORMULATION OF THE APPROXIMATE ANALYSIS

Based on the reasoning outlined in Section I, approximate solutions for the case of the decaying shock wave, Fig. 2, will be formulated for "Range II" of the material parameters, i.e., according to Eqs. (72) and (111) of [1]

$$-2 + \frac{3}{\sqrt{2(1+\nu)}} < \sqrt{3}\,\alpha < \frac{1-2\nu}{1+\nu} \tag{11}$$

This is achieved by assuming that plastic deformations occur in any element only at the time of the passing of the plastic shock front, Fig. 7, while stress changes thereafter are elastic. The stresses ahead of the shock front vanish identically, while the applicable elastic relations between stress rates and strain rates for the present case of plane strain are

$$\dot{\epsilon}_x = \frac{\partial \dot{u}}{\partial x} = \frac{1}{E}\left[\dot{\sigma}_x - \nu\,\dot{\sigma}_y - \nu\,\dot{\sigma}_z\right] = \left(\frac{1-\nu^2}{E}\right)\left[\dot{\sigma}_x - \frac{\nu}{1-\nu}\,\dot{\sigma}_y\right] \tag{12}$$

$$\dot{\epsilon}_y = \frac{\partial \dot{v}}{\partial y} = \frac{1}{E}\left[-\nu\,\dot{\sigma}_x + \dot{\sigma}_y - \nu\,\dot{\sigma}_z\right] = \left(\frac{1-\nu^2}{E}\right)\left[-\frac{\nu}{1-\nu}\,\dot{\sigma}_x + \dot{\sigma}_y\right] \tag{13}$$

$$\dot{\epsilon}_z = 0 = \frac{1}{E}\left[-\nu\,\dot{\sigma}_x - \nu\,\dot{\sigma}_y + \dot{\sigma}_z\right] \tag{14}$$

$$\dot{\epsilon}_{xy} = \frac{1}{2}\left[\frac{\partial \dot{u}}{\partial y} + \frac{\partial \dot{v}}{\partial x}\right] = \frac{1}{2G}\,\dot{\tau} \tag{15}$$

where σ_x , σ_y , σ_z , τ are the stresses, while u, v, are the displacements in the x and y directions, respectively. In addition, the equations of motion

$$\frac{\partial \sigma_x}{\partial x} + \frac{\partial \tau}{\partial y} = \rho\,\frac{\partial \dot{u}}{\partial t} \tag{16}$$

$$\frac{\partial \tau}{\partial x} + \frac{\partial \sigma_y}{\partial y} = \rho\,\frac{\partial \dot{v}}{\partial t} \tag{17}$$

must be satisfied. Equations (12, 13, 15) may be integrated with respect to time, requiring the addition of arbitrary functions $f_1(x,y)$ of x and y,

$$\frac{\partial u}{\partial x} = \frac{1-\nu^2}{E}\left[\sigma_x - \frac{\nu}{1-\nu}\sigma_y\right] + f_1(x,y) \tag{18}$$

$$\frac{\partial v}{\partial y} = \frac{1-\nu^2}{E}\left[-\frac{\nu}{1-\nu}\sigma_x + \sigma_y\right] + f_2(x,y) \tag{19}$$

$$\frac{1}{2}\left[\frac{\partial u}{\partial y} + \frac{\partial v}{\partial x}\right] = \frac{1}{2G}\tau + f_3(x,y) \tag{20}$$

while Eq. (14) after integration may be written

$$\sigma_z = \nu(\sigma_x + \sigma_y) + f_o(x,y) \tag{21}$$

The last equation is the only relation containing σ_z, and simply defines this quantity. It is noted that the arbitrary functions f_1, f_2 and f_3 are not entirely "arbitrary", but are related by a compatibility relation, as may be seen by eliminating u and v from Eqs. (18), (19) and (20).

The solution to the differential equations (16-20) may be expressed in terms of potentials Φ and Ψ which satisfy the wave equations

$$\Phi_{xx} + \Phi_{yy} = \frac{1}{c_p^2}\Phi_{tt} \tag{22}$$

$$\Psi_{xx} + \Psi_{yy} = \frac{1}{c_s^2}\Psi_{tt} \tag{23}$$

Subscripts on potentials indicate derivatives. In terms of these potentials and of two arbitrary functions g_1 and g_2 of x and y the displacements become

$$u = \Phi_x - \Psi_y + g_1(x,y) \tag{24}$$

$$v = \Phi_y + \Psi_x + g_2(x,y) \tag{25}$$

while the velocities $\dot{u}$ and $\dot{v}$ are

$$\dot{u} = \dot{\Phi}_x - \dot{\Psi}_y \tag{26}$$

$$\dot{v} = \dot{\Phi}_y + \dot{\Psi}_x \tag{27}$$

the stresses are

$$\sigma_x = 2G \left[\frac{1-\nu}{1-2\nu} \Phi_{xx} + \frac{\nu}{1-2\nu} \Phi_{yy} - \Psi_{xy} \right] \tag{28}$$

$$\sigma_y = 2G \left[\frac{\nu}{1-2\nu} \Phi_{xx} + \frac{1-\nu}{1-2\nu} \Phi_{yy} + \Psi_{xy} \right] \tag{29}$$

$$\tau = 2G \left[\Phi_{xy} + \tfrac{1}{2} (\Psi_{xx} - \Psi_{yy}) \right] \tag{30}$$

with σ_z given by Eq. (21).

Substitution of Eqs. (24-25) and (28-30) into Eqs. (18-20) furnishes relations between the three "arbitrary" functions f_1, f_2 and f_3, and the two functions g_1 and g_2, i.e.,

$$f_1 = \frac{\partial g_1}{\partial x} \quad , \quad f_2 = \frac{\partial g_2}{\partial y} \quad , \quad f_3 = \frac{1}{2} \left(\frac{\partial g_1}{\partial y} + \frac{\partial g_2}{\partial x} \right) \tag{31}$$

These three relations and the Equations (28-30) satisfy compatibility identically, leaving the two functions $g_1(x,y)$ and $g_2(x,y)$ as arbitrary functions in lieu of the related functions f_1, f_2 and f_3.

It is now noted that the velocities $\dot{u}$ and $\dot{v}$, and the stresses σ_x, σ_y and τ in terms of the potentials Φ and Ψ have exactly the same form as in an elastic plane problem and these quantities will therefore have the same value as in an entirely elastic problem with the same boundary conditions. The plastic deformations at the shock front lead, however, to different expressions for u, v and σ_z because the functions g_1, g_2 and f_o now occur. These three arbitrary functions are determinable from conditions at the plastic front as discussed below.

Because the steady-state problem is considered, where the surface pressure is solely a function of

$$\xi = x - Vt \tag{32}$$

the solutions are only functions of ξ and y. The wave equations for the potentials then become

$$\left.\begin{aligned} \phi_{yy} &= (M^2 - 1)\,\phi_{\xi\xi} \\ \psi_{yy} &= (M_S^2 - 1)\,\psi_{\xi\xi} \end{aligned}\right\} \tag{33}$$

where

$$M = \frac{V}{c_P} \quad ; \quad M_S = \frac{V}{c_S} \tag{34}$$

Noting that the open functions f_o , g_1 and g_2 , which are not functions of t, can in the steady-state not depend on x either, the expressions for displacements and stresses become

$$u = \phi_\xi - \psi_y + g_1(y) \tag{35}$$

$$v = \phi_y + \psi_\xi + g_2(y) \tag{36}$$

$$\sigma_x = G\left[2\left(1 + \frac{\nu M^2}{1-2\nu}\right)\phi_{\xi\xi} - 2\,\psi_{\xi y}\right] \tag{37}$$

$$\sigma_y = G\left[(M_S^2 - 2)\,\phi_{\xi\xi} + 2\,\psi_{\xi y}\right] \tag{38}$$

$$\tau = G\left[2\,\phi_{\xi y} - (M_S^2 - 2)\,\psi_{\xi\xi}\right] \tag{39}$$

$$\sigma_z = \nu\,(\sigma_x + \sigma_y) + f_o(y) \tag{40}$$

To formulate the boundary conditions, expressions will be required for the normal and tangential velocities $\dot{u}_N$, $\dot{u}_T$ and the normal, tangential and shear stresses σ_N , σ_T , τ_N for planes inclined at any angle φ (see Fig. 8)

$$\frac{\dot{u}_N}{V} = \sin\varphi\, \delta_{\xi\xi} - \cos\varphi\, \delta_{\xi y} - \cos\varphi\, \gamma_{\xi\xi} - \sin\varphi\, \gamma_{\xi y} \tag{41}$$

$$\frac{\dot{u}_T}{V} = -\cos\varphi\, \delta_{\xi\xi} - \sin\varphi\, \delta_{\xi y} - \sin\varphi\, \gamma_{\xi\xi} + \cos\varphi\, \gamma_{\xi y} \tag{42}$$

$$\frac{\sigma_N}{G} = \left[M_S^2 \left(1 - \frac{1-2\nu}{1-\nu}\sin^2\varphi\right) - 2\cos 2\varphi\right] \delta_{\xi\xi} - 2\sin 2\varphi\, \delta_{\xi y} + 2\cos 2\varphi\, \gamma_{\xi y} + \left(M_S^2 - 2\right)\sin 2\varphi\, \gamma_{\xi\xi} \tag{43}$$

$$\frac{\sigma_T}{G} = \left[M_S^2 \left(1 - \frac{1-2\nu}{1-\nu}\cos^2\varphi\right) + 2\cos 2\varphi\right] \delta_{\xi\xi} + 2\sin 2\varphi\, \delta_{\xi y} - 2\cos 2\varphi\, \gamma_{\xi y} - \left(M_S^2 - 2\right)\sin 2\varphi\, \gamma_{\xi\xi} \tag{44}$$

$$\frac{\tau_N}{G} = \left(M^2 - 2\right)\sin 2\varphi\, \delta_{\xi\xi} + 2\cos 2\varphi\, \delta_{\xi y} + 2\sin 2\varphi\, \gamma_{\xi y} - \left(M_S^2 - 2\right)\cos 2\varphi\, \gamma_{\xi\xi} \tag{45}$$

To state the boundary conditions of the problem properly, and to be able to make statements on the character of the solutions, the differential equations for δ and γ must be discussed. While both differential equations are hyperbolic, the characteristics for δ are steeper than the boundary $\bar{\varphi}$ defining the plastic front, $\varphi_p < \bar{\varphi}$. The solution for δ in the region of interest, $\bar{\varphi} < \varphi < \pi$, Fig. 7, is therefore defined by statements on the boundaries $\varphi = \bar{\varphi}$ and $\varphi = \pi$. δ will be a continuous function if the prescribed conditions at the boundaries are continuous. This being the case, it will be possible to use an expansion in a Taylor series in ξ and y for a region near the origin $\xi = y = 0$.

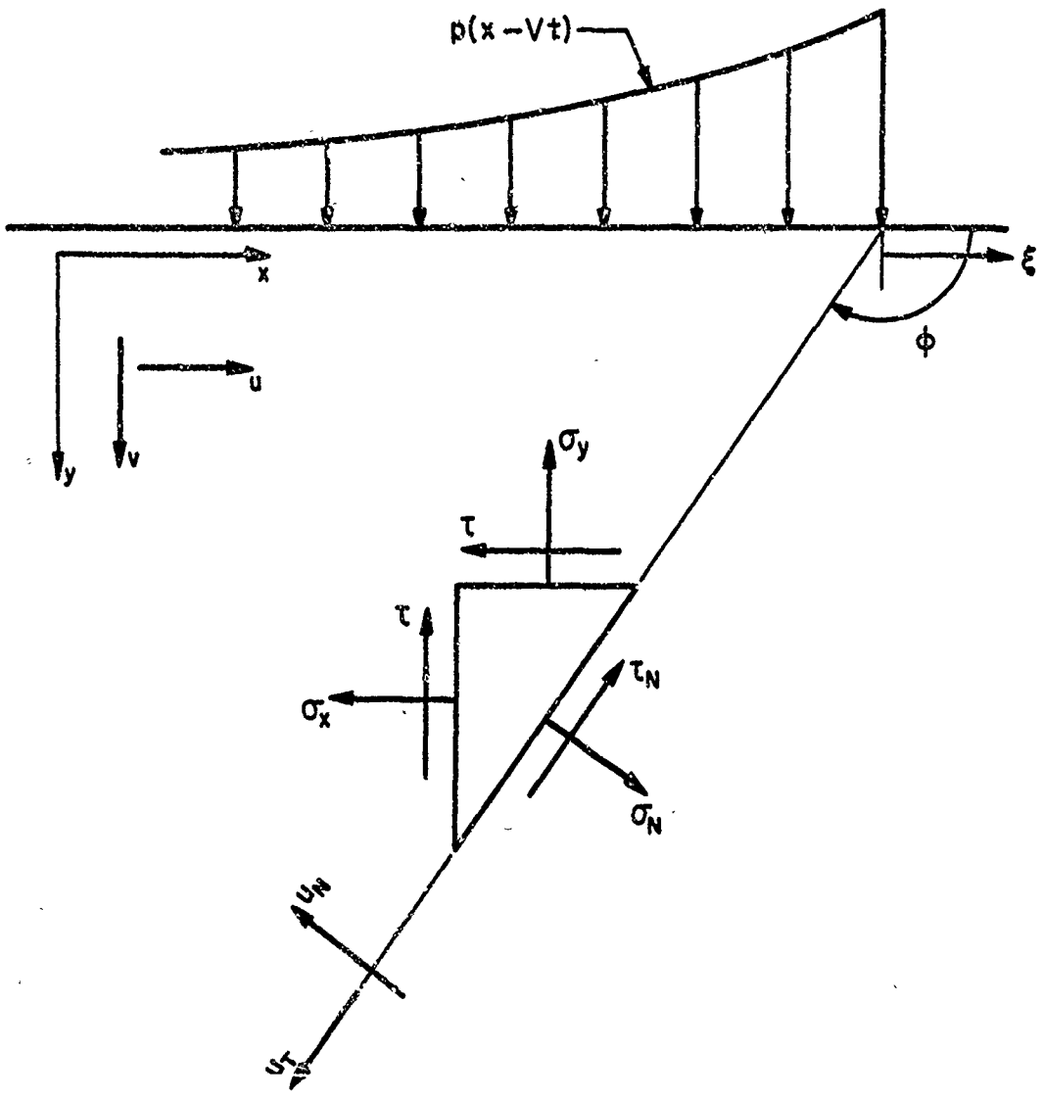

FIG. 8

On the other hand, the characteristic directions for the differential equation on Ψ are flatter than the boundary, $\varphi_s > \bar{\varphi}$. The differential equation does therefore not apply at $\varphi = \varphi_s$, and the solutions $\bar{\Psi}$ for $\varphi > \varphi_s$, and $\bar{\bar{\Psi}}$ for $\bar{\varphi} < \varphi < \varphi_s$ are not fully defined by prescriptions on $\varphi = \pi$ and $\varphi = \bar{\varphi}$. The two functions $\bar{\Psi}$ and $\bar{\bar{\Psi}}$ must, however, lead to values of stress and velocities that satisfy momentum considerations, which furnishes additional conditions for their determination. While at least some of the derivatives of $\bar{\Psi}$ and $\bar{\bar{\Psi}}$ at $\varphi = \bar{\varphi}$ will not be continuous, each of these potentials in its region will be continuous, and each of the potentials can again be expanded in a Taylor series.

The functions Ψ, $\bar{\Psi}$ and $\bar{\bar{\Psi}}$ are then subject to the following conditions. On the surface the normal and tangential stresses are prescribed. Thus for an exponentially decaying surface load,

<u>at $y = 0$, $\xi < 0$</u>

$$\sigma_y = - p_o e^{\mu \xi} \qquad (\mu > 0) \tag{46}$$

$$\tau = 0 \tag{47}$$

At the plastic front $\varphi = \bar{\varphi}$ conservation of momentum requires

<u>at $\varphi = \bar{\varphi}$</u>

$$\sigma_N = \rho \bar{c} \dot{u}_N \tag{48}$$

$$\tau_N = 0 \tag{49}$$

where $\bar{c}$, $\bar{\varphi}$ are given by Eqs. (4) and (5), respectively. In addition the yield condition must be satisfied at the plastic front so that the stresses σ_T and σ_z are related to σ_N

at $\varphi = \bar{\varphi}$

$$\sigma_T = \left(\frac{1 - \alpha\sqrt{3}}{1 + 2\alpha\sqrt{3}}\right)\sigma_N \tag{50}$$

$$\sigma_z = \left(\frac{1 - \alpha\sqrt{3}}{1 + 2\alpha\sqrt{3}}\right)\sigma_N \tag{51}$$

Due to the fact that different expressions $\bar{\Psi}$ and $\bar{\bar{\Psi}}$ for the solution of the second of Eqs. (33) will be used, it is necessary to consider additional conditions at the location $\varphi = \varphi_S$. Momentum considerations require that discontinuities in the shear stress τ_N and the tangential component of the velocity $\dot{u}_T$ are proportional. Using the symbols $\Delta\tau_N$, etc. for the discontinuities

at $\varphi = \varphi_S$

$$\Delta\tau_N = \rho\, c_S\, \Delta\dot{u}_T \tag{52}$$

while all the normal and tangential stresses and the normal velocity at $\varphi = \varphi_S$ must be continuous

at $\varphi = \varphi_S$

$$\Delta\sigma_N = 0 \tag{53}$$

$$\Delta\sigma_T = 0 \tag{54}$$

$$\Delta\sigma_z = 0 \tag{55}$$

$$\Delta\dot{u}_N = 0 \tag{56}$$

The above equations complete the available conditions for the determination of the potentials Φ, $\bar{\Psi}$ and $\bar{\bar{\Psi}}$. After the potentials are obtained the arbitrary function $f_o(y)$ appearing in Eq. (40) can be obtained from Eq. (51). The arbitrary functions $g_1(y)$ and $g_2(y)$ in Eqs. (35) and (36) are defined by the fact that the displacements must vanish at the plastic front

at $\varphi = \bar{\varphi}$

$$u = v = 0 \tag{57}$$

SECTION III

SOLUTION OF THE DIFFERENTIAL EQUATIONS BY TAYLOR SERIES.

The differential equations for the potentials to be solved are

$$\phi_{yy} - (M^2 - 1)\,\phi_{\xi\xi} = 0 \tag{58}$$

$$\left.\begin{aligned} \bar{\psi}_{yy} - (M_S^2 - 1)\,\bar{\psi}_{\xi\xi} &= 0 \\ \bar{\bar{\psi}}_{yy} - (M_S^2 - 1)\,\bar{\bar{\psi}}_{\xi\xi} &= 0 \end{aligned}\right\} \tag{59}$$

The boundary conditions, Eqs. (46-47) on the surface give

<u>at $y = 0$, $\xi < 0$</u>

$$(M_S^2 - 2)\,\phi_{\xi\xi} + 2\,\bar{\bar{\psi}}_{\xi y} = -\frac{p_o}{G}\,e^{\mu\xi} \tag{60}$$

$$2\,\phi_{\xi y} - (M_S^2 - 2)\,\bar{\bar{\psi}}_{\xi\xi} = 0 \tag{61}$$

While the conditions, Eqs. (48-50) at the plastic front give three equations

<u>at $y = \xi \tan \bar{\varphi}$</u>

$$[M_S^2 - 2 + \sin^2\bar{\varphi}\,(4 - 2M^2 - M_S^2)]\,\phi_{\xi\xi} + \left(\frac{M_S^2 - 4}{2}\right)\sin 2\bar{\varphi}\,\phi_{\xi y} +$$

$$+ [2 + (M_S^2 - 4)\sin^2\bar{\varphi}]\,\bar{\psi}_{\xi y} + \left(\frac{3M_S^2 - 4}{2}\right)\sin 2\bar{\varphi}\,\bar{\psi}_{\xi\xi} = 0 \tag{62}$$

$$(M^2 - 2)\sin 2\bar{\varphi}\,\phi_{\xi\xi} + 2\cos 2\bar{\varphi}\,\phi_{\xi y} + 2\sin 2\bar{\varphi}\,\bar{\psi}_{\xi y} - (M_S^2 - 2)\cos 2\bar{\varphi}\,\bar{\psi}_{\xi\xi} = 0 \tag{63}$$

$$2\left[\cos 2\bar{\varphi} + (M_S^2 - M^2)\left(\frac{1 + 2\alpha\sqrt{3}}{2 + \alpha\sqrt{3}}\right) - \frac{1}{2}M_S^2 + M^2\sin^2\bar{\varphi}\right]\phi_{\xi\xi} +$$

$$+ 2\sin 2\bar{\varphi}\,\phi_{\xi y} - 2\cos 2\bar{\varphi}\,\bar{\bar{\psi}}_{\xi y} - (M_S^2 - 2)\sin 2\bar{\varphi}\,\bar{\psi}_{\xi\xi} = 0 \tag{64}$$

Finally, the five conditions, Eqs. (52-56) at the S-front lead to only one condition

at $y = \xi \tan \varphi_S$

$$(\bar{\Psi}_{\xi\xi} - \bar{\bar{\Psi}}_{\xi\xi}) + \tan \varphi_S \, (\bar{\Psi}_{\xi y} - \bar{\bar{\Psi}}_{\xi y}) = 0 \tag{65}$$

The surface load is now expanded in a series in ξ

$$p_o e^{\mu \xi} = p_o \sum_{m=0}^{\infty} \frac{1}{m!} \mu^m \xi^m \tag{66}$$

applicable for $\xi < 0$, while the potentials Φ, $\bar{\Psi}$ and $\bar{\bar{\Psi}}$ are expanded in double series

$$\begin{bmatrix} \Phi \\ \bar{\Psi} \\ \bar{\bar{\Psi}} \end{bmatrix} = \sum_{i,j} \begin{bmatrix} a_{i,j} \\ b_{i,j} \\ c_{i,j} \end{bmatrix} \xi^i \, y^j \tag{67}$$

The differential equations and the conditions, Eqs. (58-65) are homogeneous, i.e., they contain consistently only second derivatives of Φ, $\bar{\Psi}$ and $\bar{\bar{\Psi}}$ with respect to ξ and y, so that the recurrence equations for the values a, b, c couple coefficients only for which i+j has the same value. In view of Eq. (66), these terms couple only with the term $m = i+j-2$ of the expression for the surface load. The potentials may therefore be written as a series of polynomials

$$\Phi = \sum_{m=0}^{\infty} \Phi^{(m)} \qquad \Phi^{(m)} = \sum_{i=0}^{m+2} a_i^{(m)} \xi^i \, y^{m+2-i} \tag{68}$$

$$\bar{\Psi} = \sum_{m=0}^{\infty} \bar{\Psi}^{(m)} \qquad \bar{\Psi}^{(m)} = \sum_{i=0}^{m+2} b_i^{(m)} \xi^i \, y^{m+2-i} \tag{69}$$

$$\bar{\bar{\Psi}} = \sum_{m=0}^{\infty} \bar{\bar{\Psi}}^{(m)} \qquad \bar{\bar{\Psi}}^{(m)} = \sum_{i=0}^{m+2} c_i^{(m)} \xi^i \, y^{m+2-i} \tag{70}$$

The case m = 0 corresponds to the step load and, while quite simple, is treated differently, see Appendix I. For values $m \geq 1$ there are (3m + 9) unknown coefficients. Substituting the second derivatives of Eqs. (68-70) into Eqs. (60-65) yields six equations:

$$(M_S^2 - 2)(m + 2)(m + 1)\, a_{m+2} + 2(m + 1)\, c_{m+1} = - \frac{p_o\, \mu^m}{G\, m!} \tag{71}$$

$$2(m + 1)\, a_{m+1} - (M_S^2 - 2)(m + 2)(m + 1)\, c_{m+2} = 0 \tag{72}$$

$$\sum_{j=1}^{m+2} (b_j - c_j)\, j\, (\tan \varphi_S)^{m+2-j} = 0 \tag{73}$$

$$(m + 2)(m + 1) \left[N_1 a_{m+2} + N_4 b_{m+2} \right] + (m + 1)(\tan \bar{\varphi})^m \left[N_2 a_1 + N_3 b_1 \right] +$$

$$+ \sum_{j=2}^{m+1} (m + 3 - j)(\tan \bar{\varphi})^{j-1} \left\{ \left[(m + 2 - j)\, N_1 + (j - 1) \cot \bar{\varphi}\, N_2 \right] a_{m+3-j} + \right.$$

$$\left. + \left[(m + 2 - j)\, N_4 + (j - 1) \cot \bar{\varphi}\, N_3 \right] b_{m+3-j} \right\} = 0 \tag{74}$$

$$(m + 2)(m + 1) \left[N_5 a_{m+2} + N_8 b_{m+2} \right] + (m + 1)(\tan \bar{\varphi})^m \left[N_6 a_1 + N_7 b_1 \right] +$$

$$+ \sum_{j=2}^{m+1} (m + 3 - j)(\tan \bar{\varphi})^{j-1} \left\{ \left[(m + 2 - j)\, N_5 + (j - 1) \cot \bar{\varphi}\, N_6 \right] a_{m+3-j} + \right.$$

$$\left. + \left[(m + 2 - j)\, N_8 + (j - 1) \cot \bar{\varphi}\, N_7 \right] b_{m+3-j} \right\} = 0 \tag{75}$$

$$(m+2)(m+1)\left[N_9 a_{m+2} + N_{10} b_{m+2}\right] + (m+1)(\tan\bar{\varphi})^m \left[N_7 a_1 - N_6 b_1\right] +$$

$$+ \sum_{j=2}^{m+1} (m+3-j)(\tan\bar{\varphi})^{j-1} \left\{ \left[(m+2-j)\, N_9 + (j-1)\, N_7 \cot\bar{\varphi}\right] a_{m+3-j} + \right.$$

$$\left. + \left[(m+2-j)\, N_{10} - (j-1)\, N_6 \cot\bar{\varphi}\right] b_{m+3-j} \right\} = 0 \qquad (76)$$

where

$$\left.\begin{aligned}
N_1 &= M_S^2 - 2 + \sin^2\bar{\varphi}\,(4 - 2M^2 - M_S^2) \\
N_2 &= -\left(\frac{M_S^2 - 4}{2}\right)\sin 2\bar{\varphi} \\
N_3 &= 2 + (M_S^2 - 4)\sin^2\bar{\varphi} \\
N_4 &= \left(\frac{3M_S^2 - 4}{2}\right)\sin 2\bar{\varphi} \\
N_5 &= (M^2 - 2)\sin 2\bar{\varphi} \\
N_6 &= 2\cos 2\bar{\varphi} \\
N_7 &= 2\sin 2\bar{\varphi} \\
N_8 &= -(M_S^2 - 2)\cos 2\bar{\varphi} \\
N_9 &= 2\left[\cos 2\bar{\varphi} + (M_S^2 - M^2)\left(\frac{1 + 2\varpi\sqrt{3}}{2 + \varpi\sqrt{3}}\right) - \frac{1}{2}M_S^2 + M^2\sin^2\bar{\varphi}\right] \\
N_{10} &= -(M_S^2 - 2)\sin 2\bar{\varphi}
\end{aligned}\right\} \qquad (77)$$

Substituting Eqs. (68-70) into the wave equations, and equating coefficients of like powers of ξ and y, yields (3m + 3) recurrence equations

$$
\left.
\begin{aligned}
a_{m-2q+2} &= (M^2 - 1)^q \, a_{m+2} \prod_{k=1}^{q} P_{m,k} \\
a_{m-2q+1} &= (M^2 - 1)^q \, a_{m+1} \, \delta_{2q-2,m} \prod_{k=1}^{q} \bar{P}_{m,k} \\
b_{m-2q+2} &= (M_S^2 - 1)^q \, b_{m+2} \prod_{k=1}^{q} P_{m,k} \\
b_{m-2q+1} &= (M_S^2 - 1)^q \, b_{m+1} \, \delta_{2q-2,m} \prod_{k=1}^{q} \bar{P}_{m,k} \\
c_{m-2q+2} &= (M_S^2 - 1)^q \, c_{m+2} \prod_{k=1}^{q} P_{m,k} \\
c_{m-2q+1} &= (M_S^2 - 1)^q \, c_{m+1} \, \delta_{2q-2,m} \prod_{k=1}^{q} \bar{P}_{m,k}
\end{aligned}
\right\} \qquad (78)
$$

where

$$
\left.
\begin{aligned}
P_{m,k} &= \frac{(m + 3 - 2k)(m + 4 - 2k)}{2k(2k - 1)} \\
\bar{P}_{m,k} &= \frac{(m + 2 - 2k)(m + 3 - 2k)}{2k(2k + 1)} \\
\delta_{2q-2,m} &= \begin{cases} 1 & \text{if} \quad 2q - 2 \neq m \\ 0 & \text{if} \quad 2q - 2 = m \end{cases} \\
1 \leq q &\leq \frac{2m + 3 + (-1)^m}{4}
\end{aligned}
\right\} \qquad (79)
$$

Equations (71-76) and Eqs. (78) give the required number of $(3m + 9)$ equations for the $(3m + 9)$ unknown coefficients a_i , b_i and c_i .

Substitution of Eqs. (78) into Eqs. (71) to (76) reduces the system to a set of six linear, nonhomogeneous, simultaneous equations, involving only the unknowns a_{m+2} , a_{m+1} , b_{m+2} , b_{m+1} , c_{m+2} , c_{m+1} . After solving for these values, the stresses, velocities and displacements for each of the m components of the surface load may be computed at any location (ξ,y) behind the front at $\bar{\varphi}$. As an illustration, the details for the case $m = 1$ are written out in full in Appendix II.

SECTION IV

NUMERICAL RESULTS AND DISCUSSION.

Numerical results from the relations derived in the previous section were obtained on a digital computer, truncating the series solution by retaining only the terms up to, and including $n = 5$. The stresses found are presented in Table II - XII and in the accompanying figures, for the values $V/c_p = 2$ and 5 for combinations of the parameters $\alpha = 0.10, 0.20$, $\nu = 0.125, 0.25, 0.333$. In addition the case $V/c_p = 2$, $\alpha = \nu = 0.05$, which lies very close to the limit between Ranges II and III, is also given. The combinations of parameters for which results are available are marked in Fig. 3.

The neglect of a plastic region, which may occur between the S-front and the surface, restricts the applicability of the resulting approximate solutions to distances from the front of the applied load where the ratio n, Eq. (8), exceeds unity only moderately. To check this matter the Tables indicate the value n for all points where stresses are listed. However, the truncation of the series further limits the validity of the results to $|\mu\xi| < 1.5$. The truncation at value $n = 5$ became necessary, because for larger values accuracy troubles developed in the computations. The numerical results presented contain, for each combination of parameters, only the range where the approximate solution is meaningful, allowing for both approximations.

1. Discussion of typical results for $V/c_p = 2$

The case $\alpha = 0.10$, $\nu = 0.125$, $V/c_p = 2.0$ is typical and is therefore selected for discussion. Figure 9 shows the nondimensional history of the principal stress σ_1 on the surface $y = 0$, and for two values of the depth, $\mu y = 0.05$ and 0.40. The values σ_1 are plotted against $\mu\xi \tan\bar{\varphi} = |\mu Vt \tan\bar{\varphi}|$, where t is the time elapsed

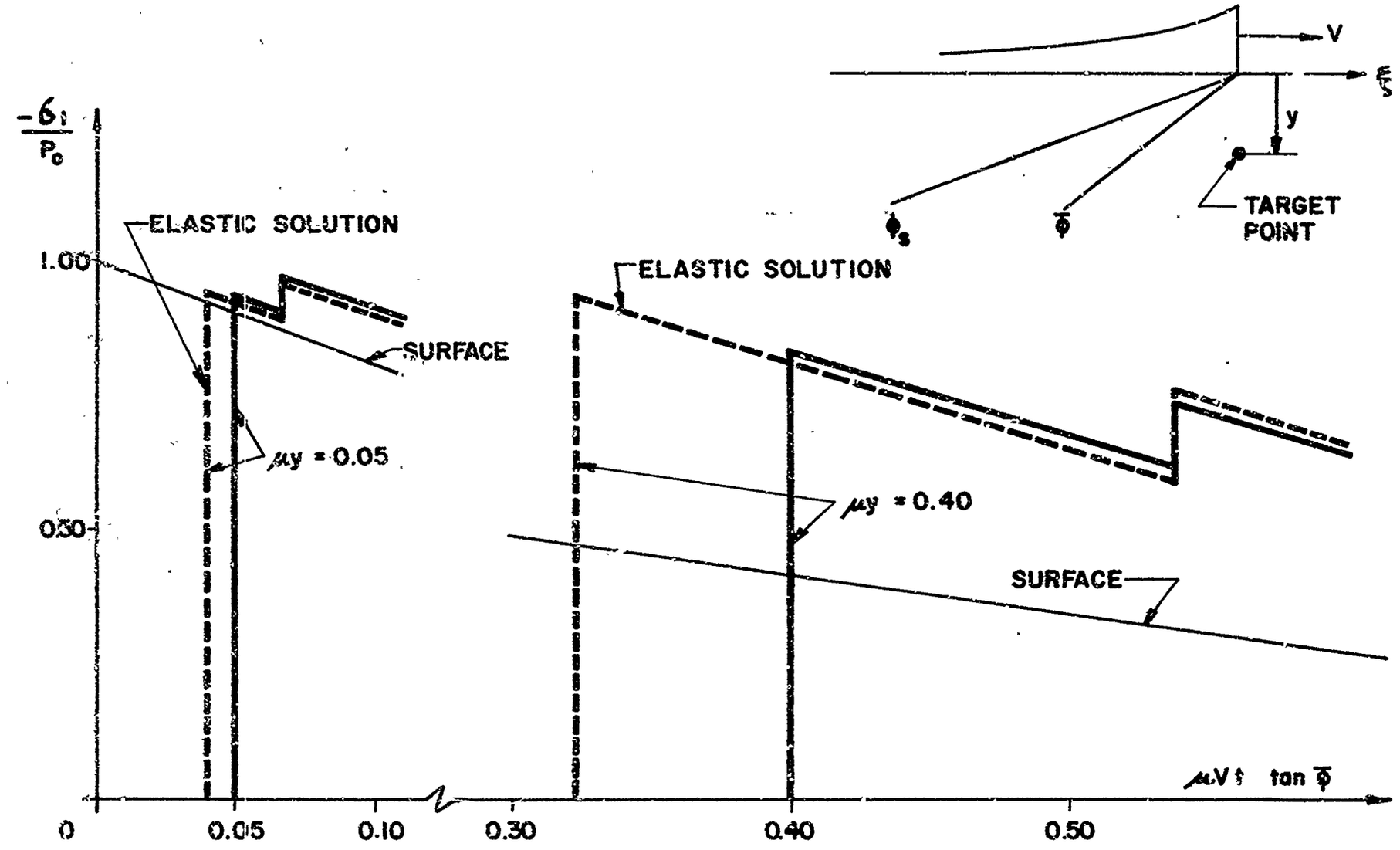

FIG. 9 RESULTS FOR $\gamma = 1.25$ $\alpha = 0.10$ $V/c_p = 2.0$

after arrival of the surface load above the target point. The curve σ_1 for $y = 0$ shows just the history of the applied load, while the other curves indicate a discontinuous increase in $(-\sigma_1)$ at the arrival of the plastic front, followed by a decrease in $(-\sigma_1)$. This is subsequently followed by a second discontinuous increase in $(-\sigma_1)$ at arrival of the S-front, followed by a gradual decrease. Attention is drawn to an important difference between the curves for $\mu y = 0.05$ and $\mu y = 0.40$. The former is representative of the situation at small depths, where the maximum value of $(-\sigma_1)$ occurs at the second peak due to the passing of the S-front. The curve for $\mu y = 0.40$ is representative of the situation at larger depths, when the first peak due to the passing of the plastic front gives the maximum value of $(-\sigma_1)$. The equivalent occurs in the case of a decaying load on an entirely elastic medium, and Fig. 9 shows the comparative histories of $(-\sigma_1)$ at the two depths $\mu y = 0.05$ and 0.40 in dashed lines. The arrival time of the first peak in the elastic cases is of course earlier, but the relative values of the first and second peaks bear the same relation as for the elastic-plastic material.

Further details for the above values of the parameters are given in Table II and its accompanying figure. Table II shows the values of the principal stresses σ_1, σ_2 in the ξ-y plane as well as the third principal stress σ_3, and the angle θ between the direction of σ_1 and the ξ axis. In addition, the values of n, indicating the violation of the yield condition, are listed. The information in Table 2 is given for a rectangular network of points, 1-10, selected such that one point at each of the depth levels falls on the plastic front. Additional points, 11 to 13, lie on the S-front. At point 1 two values for each quantity are given, because the stress field has a singularity, i.e. the values depend on the direction of approach φ, and the results differ depending on

whether $\varphi \gtrless \varphi_s$. (The two sets of values at point 1 immediately behind the front of the applied load are of course equal to those due to a step load without decay.)

The values n in the last colum of Table 2 permit evaluation of the approximation achieved. There is a moderate violation of the yield condition at point 1, n = 1.19. As mentioned above, this point represents the values due to a step load without decay, for which case results are known without approximation. To judge the seriousness of the violation expressed by $n = 1.19 > 1$ Table 1 gives the exact values of the stresses σ_i and angles θ. It is seen that the differences

TABLE I

Exact values at $\xi = y = 0$, for $\nu = 0.125$, $\alpha = 0.10$, $V/c_p = 2.0$

Location	$-\sigma_1/p_o$	$-\sigma_2/p_o$	$-\sigma_3/p_o$	θ
$\bar{\varphi} < \varphi < \varphi_s$	0.944	0.580	0.580	65.03°
$\varphi = \pi$	1.00	0.598	0.632	90.00°

in the principal stresses are not large, the maximum being 9%. The errors at the shock front are very small, less than 2%. While the values θ listed in Table 1 agree with those in Table 2, it is noted that in the exact case the value θ varies between $\varphi = \varphi_s$ and $\varphi = \pi$ from 76.76° to 90°, while the approximate value for θ in this entire range is 90°. While this difference in direction may not be of great practical importance, it is percentage-wise of the order of the error in n, and about twice as large as the error in the stresses.

Moving away from point 1 at the origin to adjacent points 2, 5, 11 at $\mu\xi = -0.215$, and to further points at $\mu\xi = -0.859$ and $\mu\xi = -1.289$ it is noted

TABLE II

Results for $\nu = 0.125$, $\alpha = 0.10$, $V/c_P = 2.0$

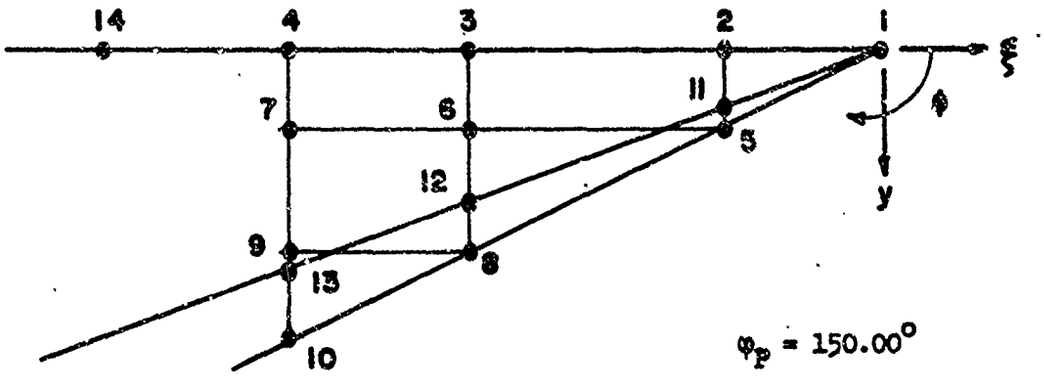

$\varphi_P = 150.00^\circ$

$\varphi_S = 160.89^\circ$

$\bar{\varphi} = 155.03^\circ$

Point	$-\mu\xi$	$\mu\eta$	$-\sigma_1/p_o$	$-\sigma_2/p_o$	$-\sigma_3/p_o$	θ°	n
1 *	0	0	0.9547	0.5862	0.5862	65.03	1.00
1 **	0	0	1.00	0.5409	0.5862	90.00	1.19
2	0.215	0	0.8067	0.5209	0.5596	90.00	0.822
3	0.859	0	0.4231	0.4738	0.5057	90.00	0.297
4	1.289	0	0.2703	0.4494	0.4836	90.00	0.952
5	0.215	0.100	0.9202	0.5651	0.5651	65.03	1.00
6	0.859	0.100	0.5178	0.4606	0.5017	100.3	0.199
7	1.289	0.100	0.3325	0.4422	0.4763	88.19	0.601
8	0.859	0.400	0.8251	0.5067	0.5067	65.03	1.00
9	1.289	0.400	0.6398	0.3640	0.4657	104.8	0.949
10	1.289	0.600	0.7679	0.4715	0.4715	65.03	1.00
11***	0.215	0.074	0.9365	0.5048	0.5632	92.59	1.17
12***	0.859	0.298	0.7867	0.4026	0.5017	100.2	1.18
13***	1.289	0.446	0.7107	0.3404	0.4659	104.6	1.24
14	1.500	0	0.2102	0.4488	0.4747	90.00	1.28

* Values at $\bar{\varphi} \leq \varphi < \varphi_S$. ** Values at $\varphi_S < \varphi \leq \pi$

*** Values at $\varphi = \varphi_S^+$. At $\varphi = \varphi_S$, $\Delta\tau = + 0.477\ p_o$.

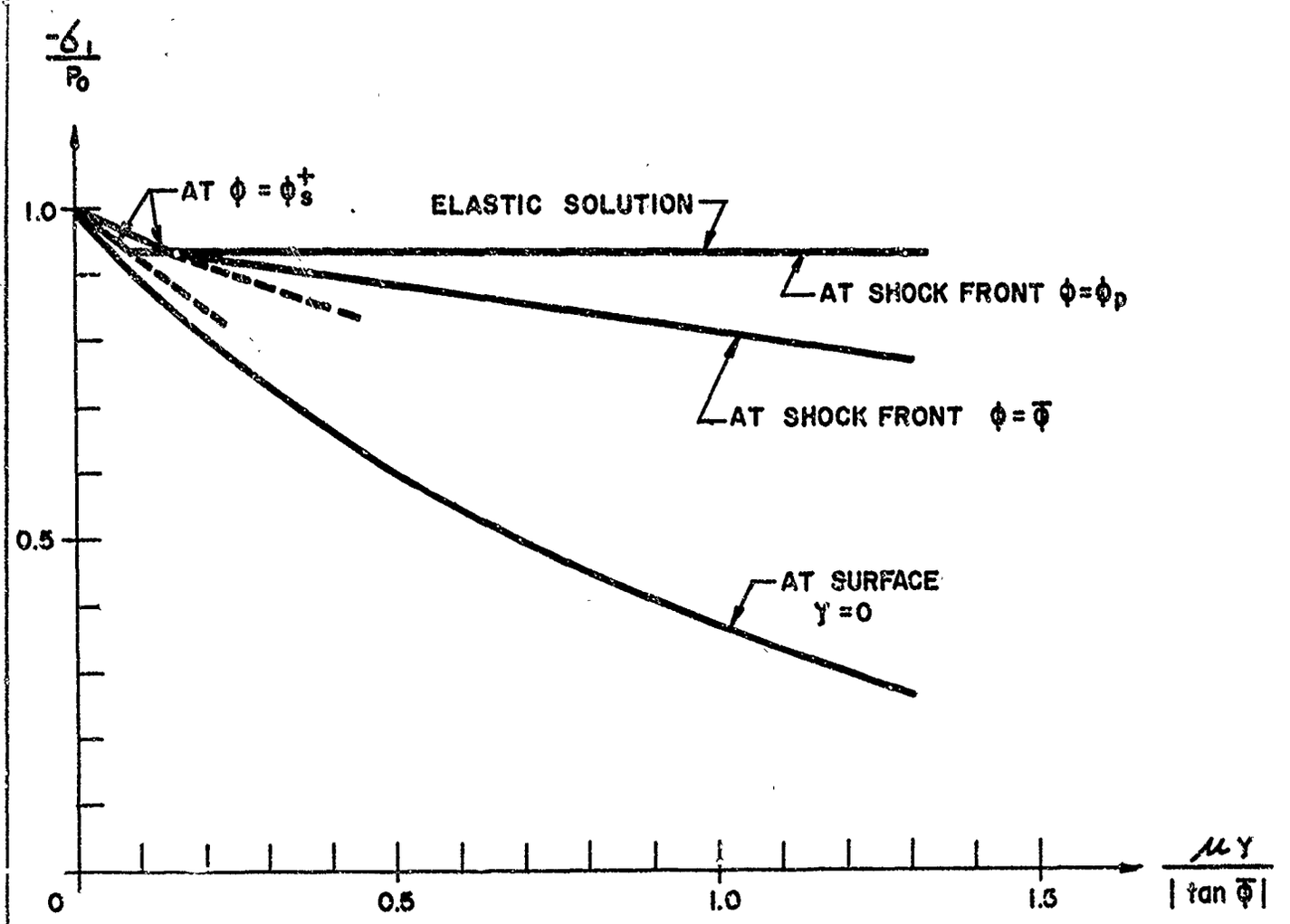

FIG. 10 PRINCIPAL STRESS σ_1 FOR
$\nu = 0.125$, $\alpha = 0.10$, $V/c_p = 2.0$

TABLE III

Results for $\nu = 0.125$, $\alpha = 0.10$, $V/c_p = 5.0$

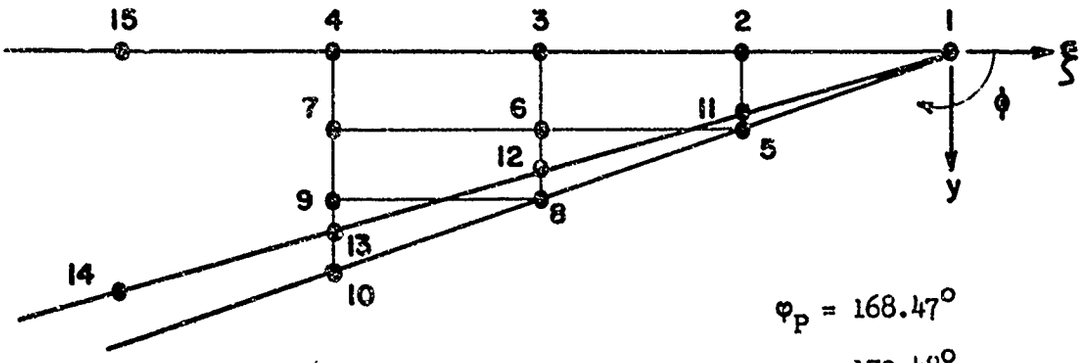

$\varphi_P = 168.47^\circ$

$\varphi_S = 172.48^\circ$

$\bar{\varphi} = 170.28^\circ$

Point	$-\mu\xi$	μy	$-\sigma_1/p_o$	$-\sigma_2/p_o$	$-\sigma_3/p_o$	ϑ°	n
1 *	0	0	0.9938	0.6103	0.6103	80.28	1.00
1 **	0	0	1.00	0.6041	0.6103	90.00	1.02
2	0.292	0	0.7469	0.5621	0.5734	90.00	0.550
3	0.876	0	0.4161	0.5018	0.5245	90.00	0.396
4	1.167	0	0.3082	0.4794	0.5082	90.00	0.835
5	0.292	0.050	0.9523	0.5848	0.5848	80.28	1.00
6	0.876	0.050	0.5455	0.4974	0.5231	55.31	0.155
7	1.167	0.050	0.4942	0.3878	0.5029	104.1	0.463
8	0.876	0.150	0.8751	0.5374	0.5374	80.28	1.00
9	1.167	0.150	0.6636	0.4924	0.5053	71.80	0.574
10	1.167	0.200	0.8391	0.5152	0.5152	80.28	1.00
11***	0.292	0.039	0.9016	0.5771	0.5813	87.86	0.904
12***	0.876	0.116	0.7393	0.5240	0.5294	79.77	0.685
13***	1.167	0.154	0.6756	0.4944	0.5058	72.94	0.606
14***	1.459	0.193	0.6250	0.4602	0.4837	64.44	0.568
15	1.459	0	0.2213	0.4599	0.4949	90.00	1.27

* Values at $\bar{\varphi} \leq \varphi < \varphi_S$ ** Values at $\varphi_S < \varphi \leq \pi$

*** Values at $\varphi = \varphi_S^+$. At $\varphi = \varphi_S$, $\Delta\tau = +0.208\ p_o$.

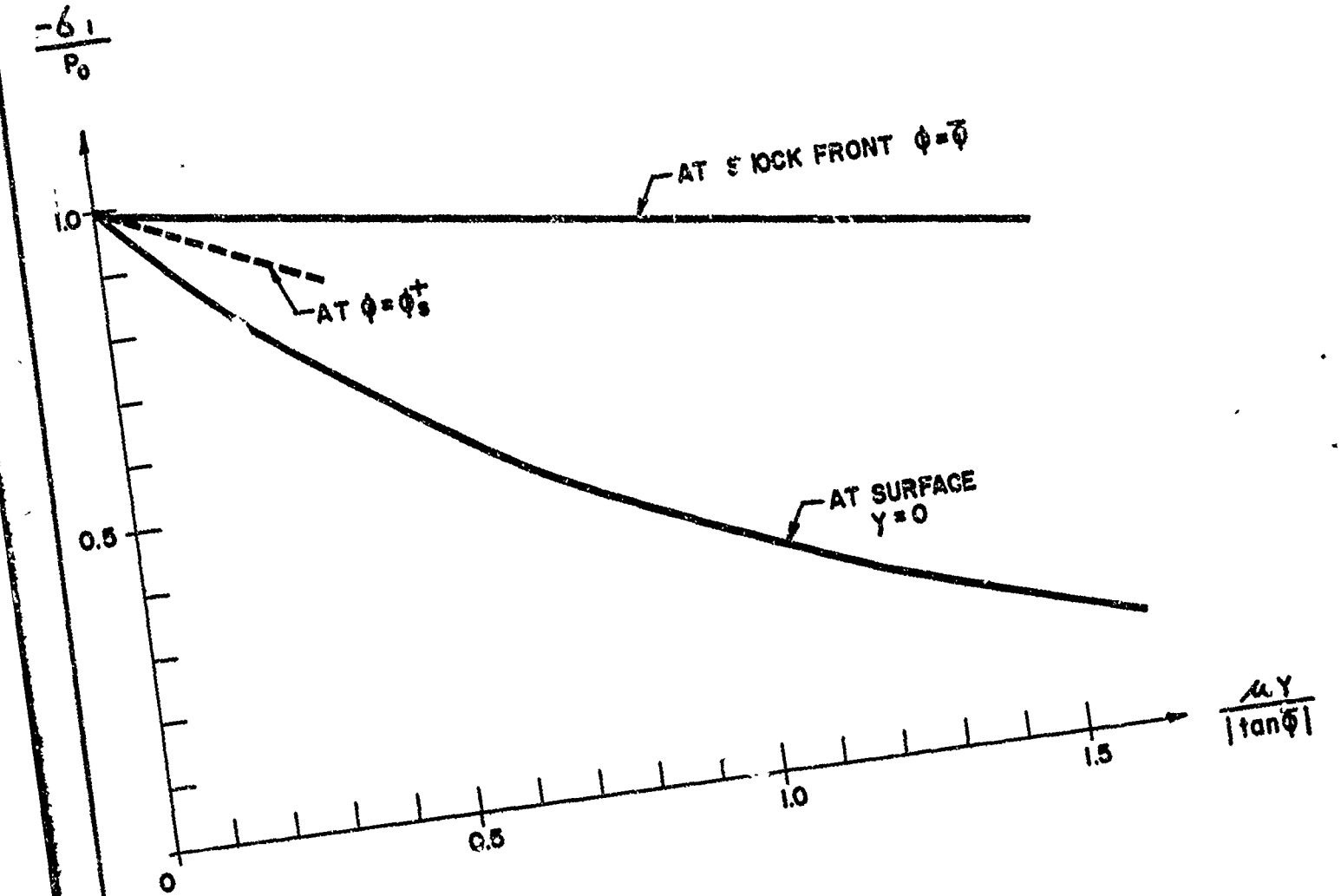

FIG. 11 PRINCIPAL STRESS σ_1 FOR $\nu = 0.125$, $\alpha = 0.10$, $V/c_p = 5.0$

TABLE IV

Results for $\nu = 0.125$, $\alpha = 0.20$, $V/c_p = 2.0$

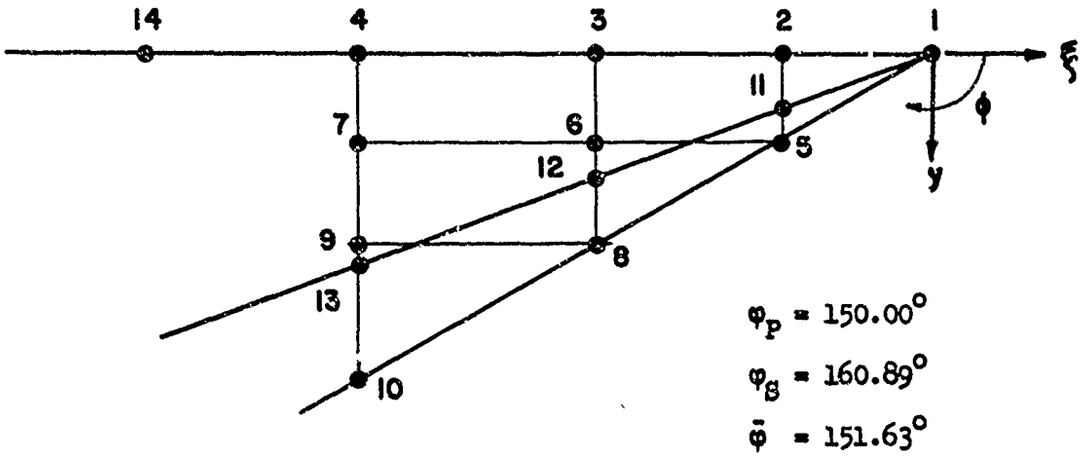

Point	$-\mu\xi$	μy	$-\sigma_1/p_o$	$-\sigma_2/p_o$	$-\sigma_3/p_o$	θ°	n
1 *	0	0	0.9403	0.3631	0.3631	61.63	1.00
1 **	0	0	1.000	0.3031	0.3631	90.00	1.16
2	0.278	0	0.7575	0.2869	0.3307	90.00	0.945
3	0.556	0	0.5737	0.2739	0.3061	90.00	0.713
4	0.926	0	0.3954	0.2607	0.2821	90.00	0.386
5	0.278	0.15	0.9241	0.3568	0.3568	61.63	1.00
6	0.556	0.15	0.7841	0.2424	0.3250	94.82	1.08
7	0.926	0.15	0.5412	0.2386	0.2942	95.80	0.750
8	0.556	0.30	0.9083	0.3507	0.3507	61.63	1.00
9	0.926	0.30	0.7516	0.1883	0.3108	99.19	1.18
10	0.926	0.50	0.8671	0.3348	0.3348	61.63	1.00
11***	0.278	0.096	0.9239	0.2650	0.3465	92.98	1.17
12***	0.556	0.192	0.8590	0.2272	0.3315	95.90	1.19
13***	0.926	0.321	0.7873	0.1782	0.3135	99.58	1.25
14	1.30	0	0.2669	0.2505	0.2648	90.00	0.057

* Values at $\bar{\varphi} \leq \varphi < \varphi_s$ ** Values at $\varphi_s < \varphi \leq \pi$

*** Values at $\varphi = \varphi_s^+$. At $\varphi = \varphi_s$, $\Delta\tau = + 0.403\ p_o$.

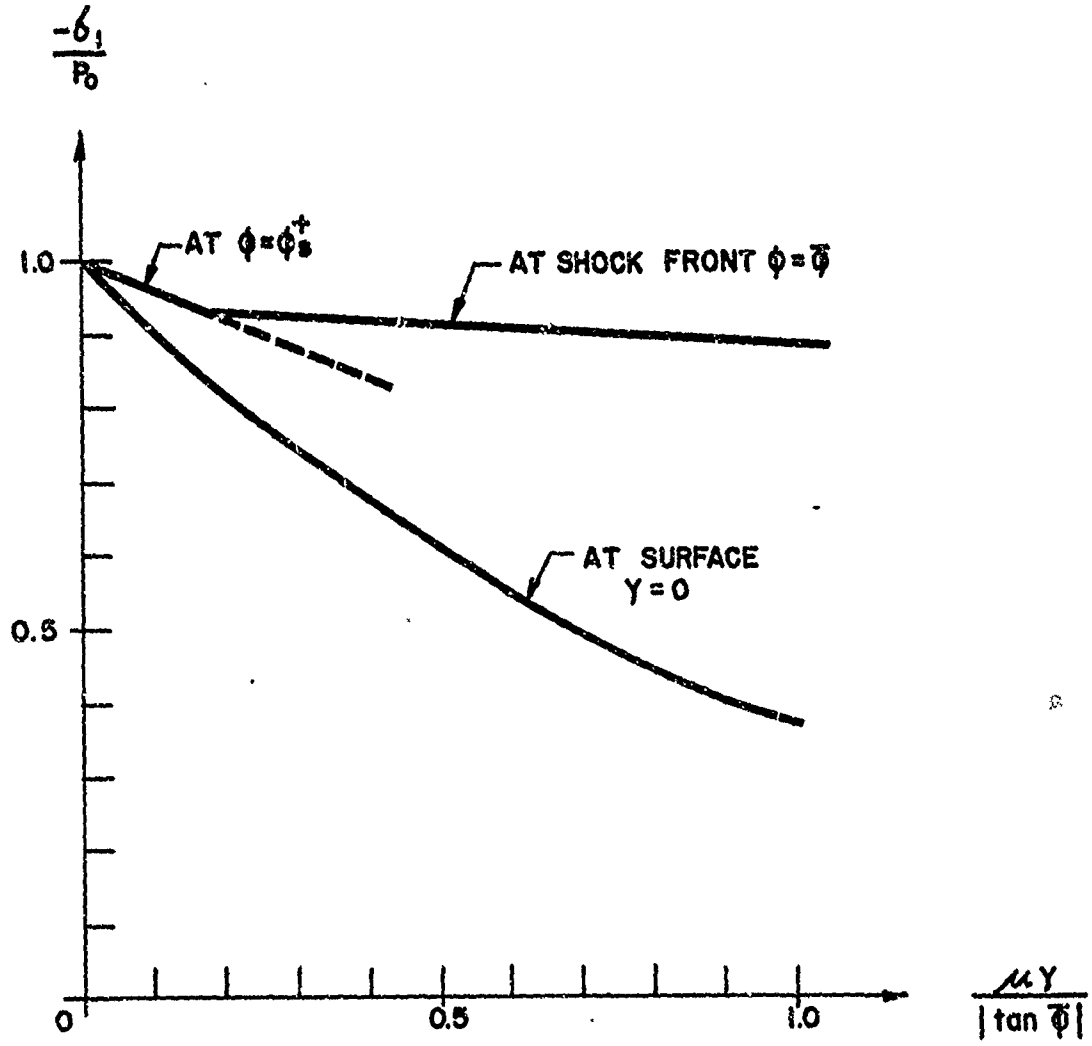

FIG. 12 PRINCIPAL STRESS σ_1 FOR
$\nu = 0.125$, $\alpha = 0.20$, $V/c_p = 2.0$

TABLE V

Results for $\nu = 0.125$, $\alpha = 0.20$, $V/c_p = 5.0$

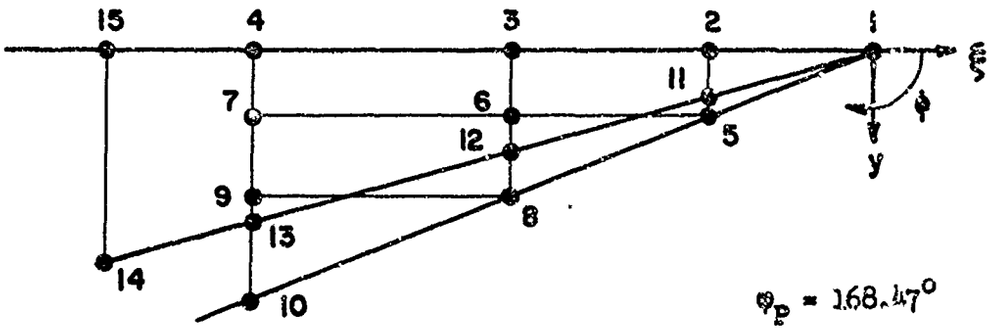

$\varphi_p = 168.47^\circ$

$\varphi_s = 172.48^\circ$

$\bar{\varphi} = 169.04^\circ$

Points	$-\mu\xi$	μy	$-\sigma_1/p_o$	$-\sigma_2/p_o$	$-\sigma_3/p_o$	θ°	n
1 *	0	0	0.9915	0.3828	0.3828	79.04	1.00
1 **	0	0	1.000	0.3743	0.3828	90.00	1.02
2	0.258	0	0.7724	0.3432	0.3505	90.00	0.838
3	0.775	0	0.4605	0.2999	0.3061	90.00	0.427
4	1.30	0	0.2669	0.2720	0.2784	90.00	0.035
5	0.258	0.05	0.9786	0.3778	0.3778	79.04	1.00
6	0.775	0.05	0.5912	0.3125	0.3212	91.61	0.647
7	1.30	0.05	0.3475	0.2799	0.2867	91.97	0.204
8	0.775	0.15	0.9533	0.3681	0.3681	79.04	1.00
9	1.30	0.15	0.5794	0.2956	0.3123	95.74	0.671
10	1.30	0.252	0.9283	0.3584	0.3584	79.04	1.00
11***	0.258	0.034	0.9159	0.3574	0.3683	91.05	0.973
12***	0.775	0.10	0.7011	0.3258	0.3414	93.49	0.864
13***	1.30	0.171	0.6500	0.2985	0.3204	96.58	0.776
14***	1.55	0.205	0.5983	0.2855	0.3105	98.39	0.728
15	1.55	0	0.1966	0.2616	0.2683	90.00	0.272

* Values at $\bar{\varphi} \leq \varphi < \varphi_s$. ** Values at $\varphi_s < \varphi \leq \pi$

*** Values at $\varphi = \varphi_s^+$. At $\varphi = \varphi_s$, $\Delta\tau = + 0.178\ p_o$.

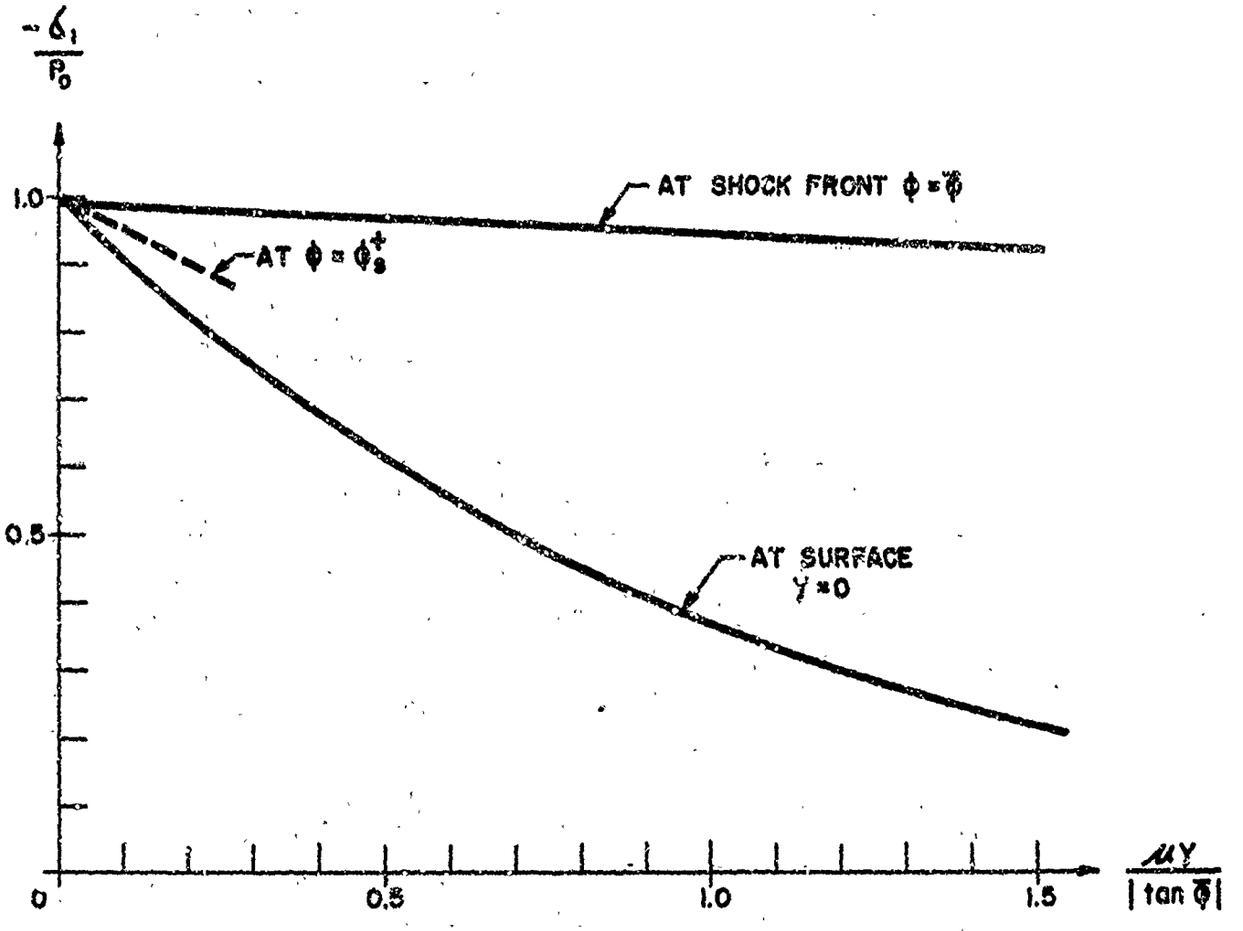

FIG. 13 PRINCIPAL STRESS σ_1 FOR
$\nu = 0.125$, $\alpha = 0.20$, $V/c_p = 5.0$

TABLE VI

Results for $\nu = 0.25$, $\alpha = 0.10$, $V/c_p = 2.0$

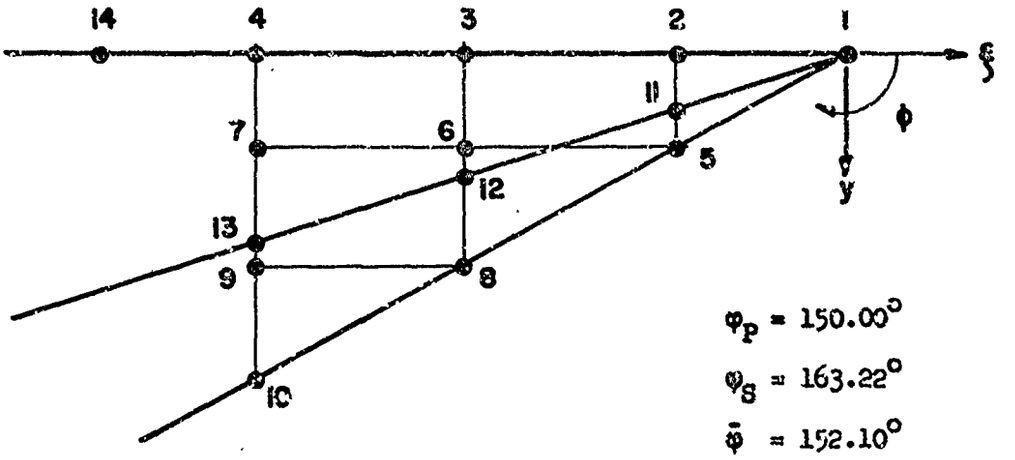

Point	$-\beta\bar{x}$	βy	$-\sigma_1/p_o$	$-\sigma_2/p_o$	$-\sigma_3/p_o$	φ°	n
1 *	0	0	0.9791	0.6012	0.6012	62.10	1.00
1 **	0	0	1.000	0.5803	0.6012	90.00	1.08
2	0.283	0	0.7533	0.5033	0.5203	90.00	0.786
3	0.756	0	0.4695	0.4135	0.4269	90.00	0.224
4	1.133	0	0.3195	0.3648	0.3772	90.00	0.286
5	0.283	0.15	0.9566	0.5874	0.5874	62.10	1.00
6	0.756	0.15	0.6444	0.4170	0.4668	100.6	0.782
7	1.133	0.15	0.4450	0.3629	0.4034	110.4	0.339
8	0.756	0.40	0.9203	0.5651	0.5651	62.10	1.00
9	1.133	0.40	0.6332	0.4645	0.4682	63.69	0.615
10	1.133	0.60	0.8923	0.5479	0.5479	62.10	1.00
11***	0.283	0.085	0.8973	0.5126	0.5559	94.91	1.07
12***	0.756	0.228	0.7668	0.4072	0.4925	102.8	1.13
13***	1.133	0.342	0.6885	0.3299	0.4501	108.3	1.24
14	1.30	0	0.2669	0.3474	0.3597	90.00	0.518

* Values at $\bar{\varphi} \leq \varphi < \varphi_S$ ** Values at $\varphi_S < \varphi \leq \pi$

*** Values at $\varphi = \varphi_S^+$. At $\varphi = \varphi_S$, $\Delta\tau = + 0.437\ p_o$.

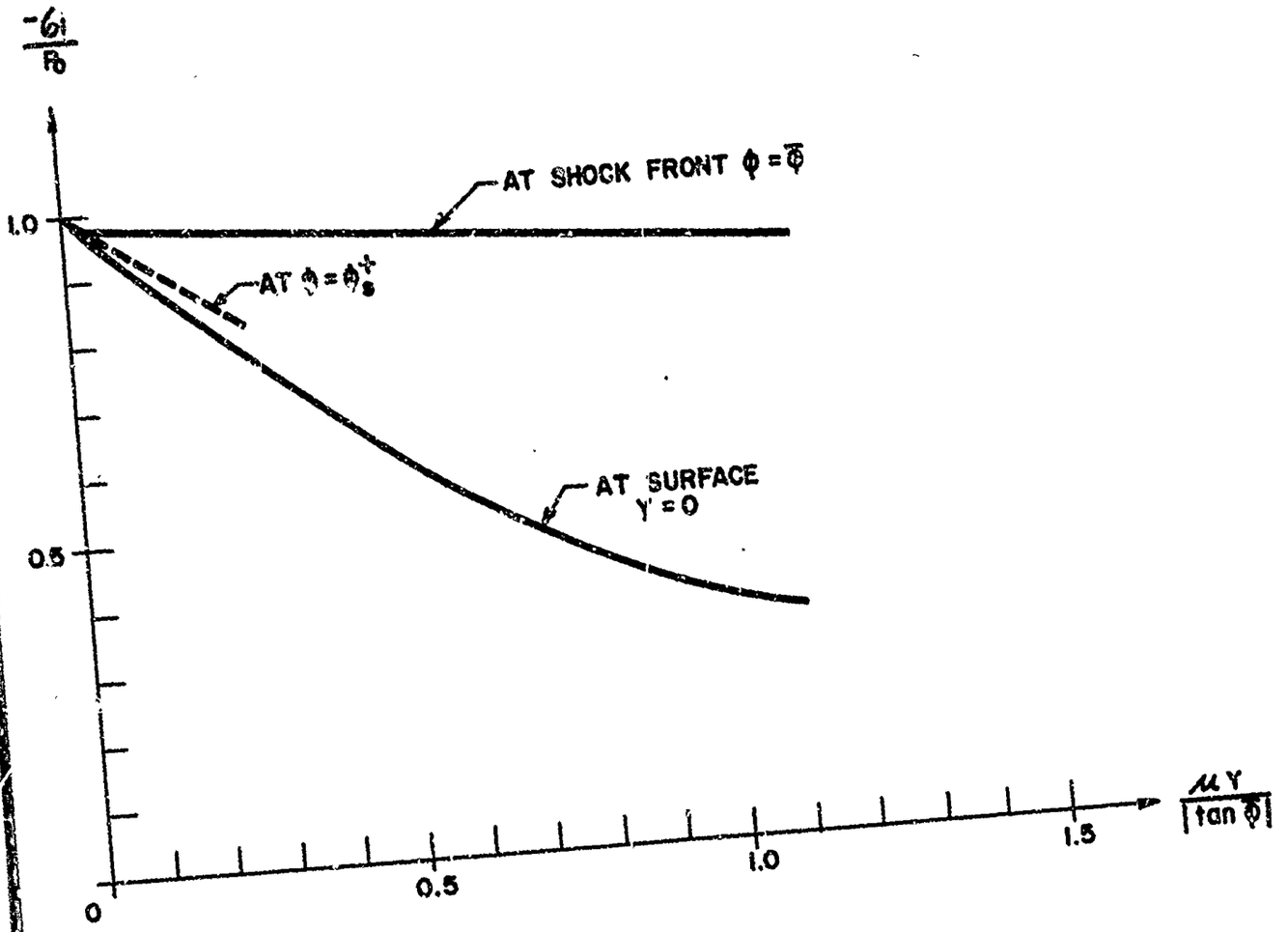

FIG. 14 PRINCIPAL STRESS σ_1 FOR
$\nu = 0.25$, $\alpha = 0.10$, $V/c_p = 2.0$

TABLE VII

Results for $\nu = 0.25$, $\alpha = 0.10$, $V/c_p = 5.0$

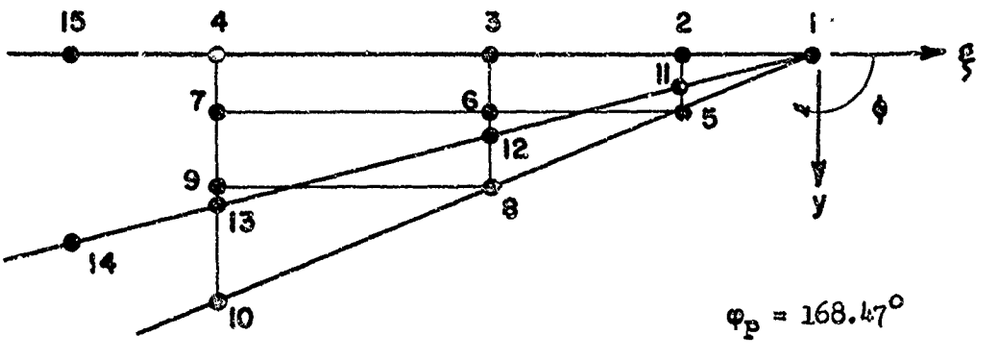

$\varphi_p = 168.47^\circ$

$\varphi_s = 173.36^\circ$

$\tilde{\varphi} = 169.21^\circ$

Point	$-\mu\xi$	μy	$-\sigma_1/p_o$	$-\sigma_2/p_o$	$-\sigma_3/p_o$	θ°	n
1 *	0	0	0.9968	0.6121	0.6121	79.21	1.00
1 **	0	0	1.000	0.6089	0.6121	90.00	1.01
2	0.262	0	0.7692	0.5313	0.5350	90.00	0.742
3	0.787	0	0.4548	0.4245	0.4297	90.00	0.124
4	1.312	0	0.2633	0.3580	0.3652	90.00	0.576
5	0.262	0.05	0.9795	0.6015	0.6015	79.21	1.00
6	0.787	0.05	0.5829	0.4614	0.4673	92.70	0.453
7	1.312	0.05	0.3810	0.3421	0.3870	90.42	0.220
8	0.787	0.15	0.9457	0.5807	0.5807	79.21	1.00
9	1.312	0.15	0.5723	0.4360	0.4512	101.0	0.512
10	1.312	0.25	0.9131	0.5607	0.5607	79.21	1.00
11***	0.262	0.031	0.8943	0.5678	0.5732	91.39	0.919
12***	0.787	0.092	0.7181	0.4970	0.5070	95.12	0.725
13***	1.312	0.153	0.5794	0.4374	0.4531	101.2	0.530
14***	1.575	0.183	0.5226	0.4106	0.4301	105.8	0.439
15	1.575	0	0.1899	0.3321	0.3404	90.00	0.981

* Values at $\tilde{\varphi} \leq \varphi < \varphi_s$. ** Values at $\varphi_s < \varphi \leq \pi$

*** Values at $\varphi = \varphi_s^+$. At $\varphi = \varphi_s$, $\Delta\tau = + 0.185\ p_o$.

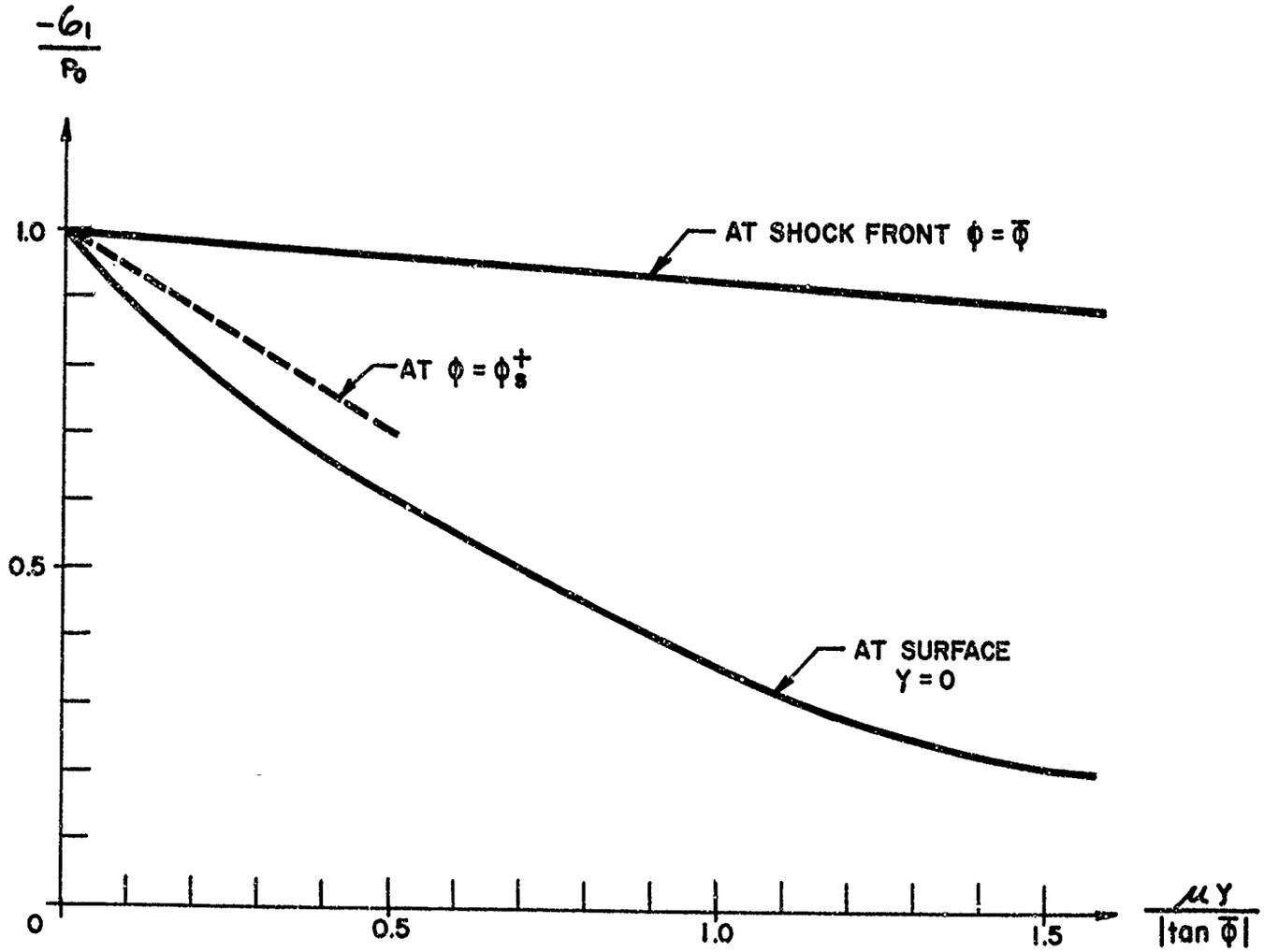

FIG. 15 PRINCIPAL STRESS σ_1 FOR
$\bar{V} = 0.25$, $\alpha = 0.10$, $V/c_p = 5.0$

TABLE VIII

Results for $\nu = 0.25$, $\alpha = 0.20$, $V/c_p = 2.0$

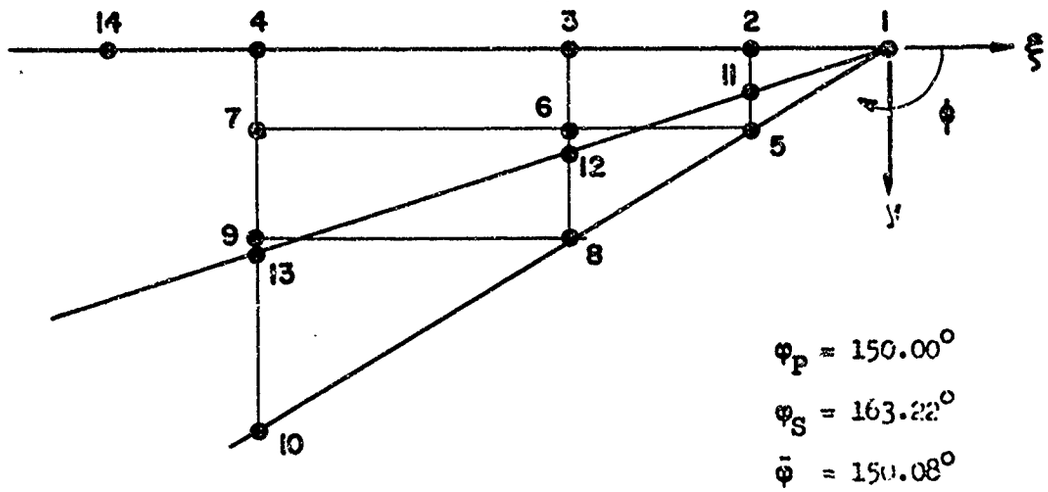

$\varphi_p = 150.00^\circ$

$\varphi_s = 163.22^\circ$

$\bar{\varphi} = 150.08^\circ$

Point	$-\mu\xi$	μy	$-\sigma_1/p_o$	$-\sigma_2/p_o$	$-\sigma_3/p_o$	θ°	n
1 *	0	0	0.9772	0.3773	0.3773	60.08	1.00
1 **	0	0	1.000	0.3545	0.3773	90.00	1.06
2	0.261	0	0.7705	0.2854	0.3027	90.00	1.01
3	0.521	0	0.5937	0.2321	0.2451	90.00	0.958
4	0.869	0	0.4189	0.1795	0.1883	90.00	0.862
5	0.261	0.15	0.9764	0.3770	0.3770	60.08	1.00
6	0.521	0.15	0.8144	0.2406	0.3024	95.85	1.16
7	0.869	0.15	0.5754	0.1854	0.2288	96.08	1.08
8	0.521	0.30	0.9755	0.3766	0.3766	60.08	1.00
9	0.869	0.30	0.6895	0.2813	0.2813	60.12	0.941
10	0.869	0.50	0.9744	0.3762	0.3762	60.08	1.00
11***	0.261	0.079	0.9056	0.2953	0.3389	93.10	1.11
12***	0.521	0.157	0.8272	0.2402	0.3055	96.10	1.17
13***	0.869	0.262	0.7402	0.1721	0.2667	99.84	1.29
14	1.30	0	0.2669	0.1337	0.1388	90.00	0.699

* Values at $\bar{\varphi} \leq \varphi < \varphi_s$. ** Values at $\varphi_s < \varphi \leq \pi$

*** Values at $\varphi = \varphi_s^+$. At $\varphi = \varphi_s$, $\Delta\tau = +0.374\ p_o$.

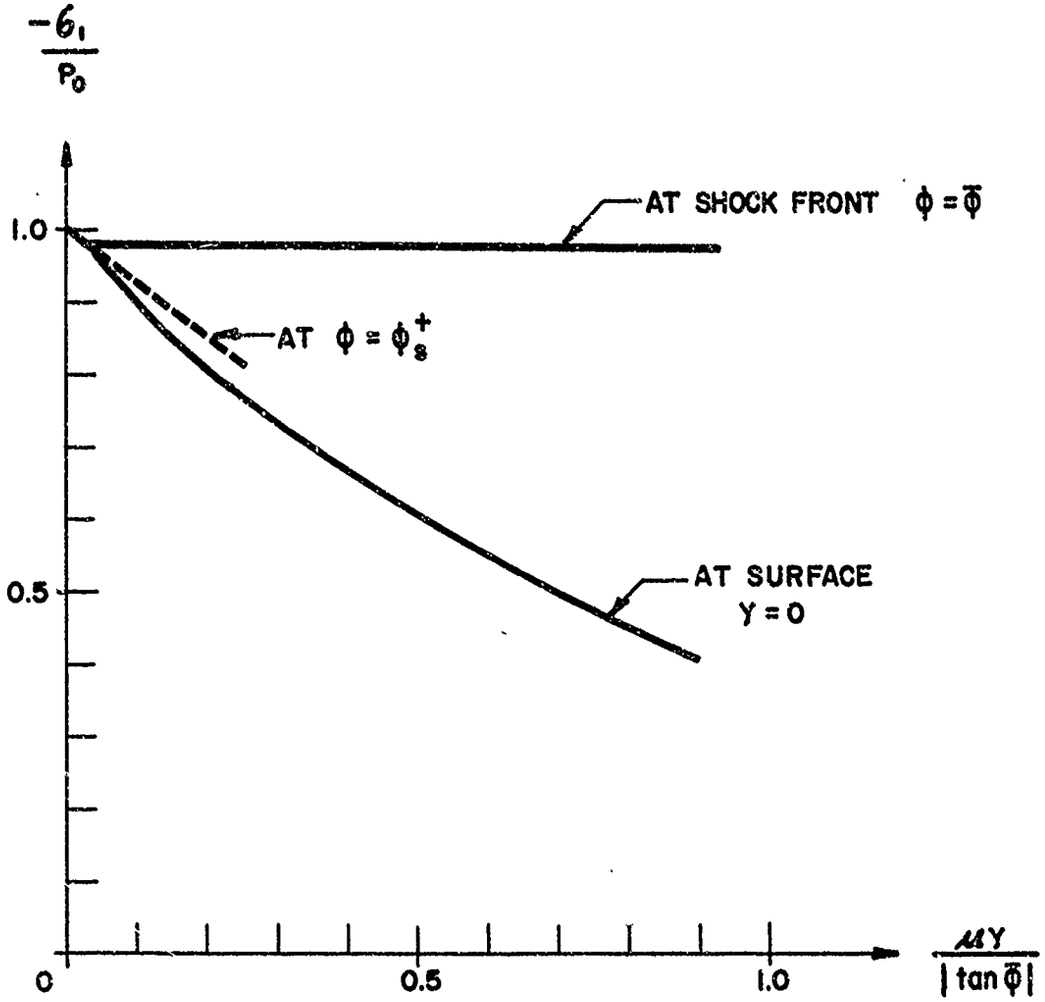

FIG. 16 PRINCIPAL STRESS σ_1 FOR
$\dot{V} = 0.25$, $\alpha = 0.20$, $\dot{V}/c_p = 2.0$

TABLE IX

Results for $\nu = 0.25$, $\alpha = 0.20$, $V/c_P = 5.0$

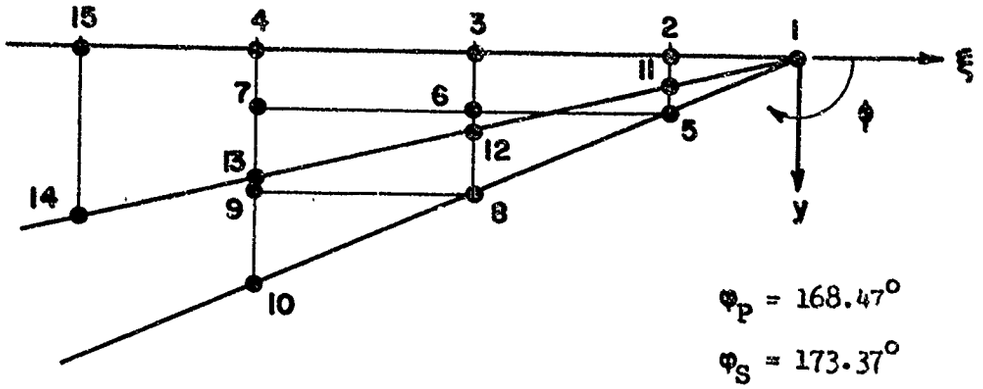

$\varphi_P = 168.47^\circ$

$\varphi_S = 173.37^\circ$

$\bar{\varphi} = 168.49^\circ$

Point	$-\mu\xi$	μy	$-\sigma_1/p_o$	$-\sigma_2/p_o$	$-\sigma_3/p_o$	θ°	n
1 *	0	0	0.9962	0.3846	0.3846	78.49	1.00
1 **	0	0	1.000	0.3808	0.3846	90.00	1.01
2	0.246	0	0.7822	0.3094	0.3123	90.00	0.969
3	0.737	0	0.4785	0.2097	0.2115	90.00	0.896
4	1.23	0	0.2889	0.1476	0.1485	90.00	0.695
5	0.246	0.05	0.9955	0.3844	0.3844	78.49	1.00
6	0.737	0.05	0.6160	0.2488	0.2556	92.52	0.937
7	1.23	0.05	0.3759	0.1723	0.1765	92.80	0.803
8	0.737	0.15	0.9942	0.3839	0.3839	78.49	1.00
9	1.23	0.15	0.6085	0.2552	0.2553	78.49	0.911
10	1.23	0.25	0.9930	0.3834	0.3834	78.49	1.00
11***	0.246	0.029	0.9021	0.3442	0.3510	91.34	1.00
12***	0.737	0.086	0.7384	0.2803	0.2941	94.42	0.993
13***	1.230	0.143	0.6088	0.2258	0.2480	98.04	0.993
14***	1.474	0.171	0.5553	0.2014	0.2285	100.1	1.00
15	1.474	0	0.2174	0.1241	0.1248	90.00	0.975

* Values at $\bar{\varphi} \leq \varphi < \varphi_S$ ** Values at $\varphi_S < \varphi \leq \pi$

*** Values at $\varphi = \varphi_S^+$. At $\varphi =$, $\Delta\tau = + 0.158\ p_o$.

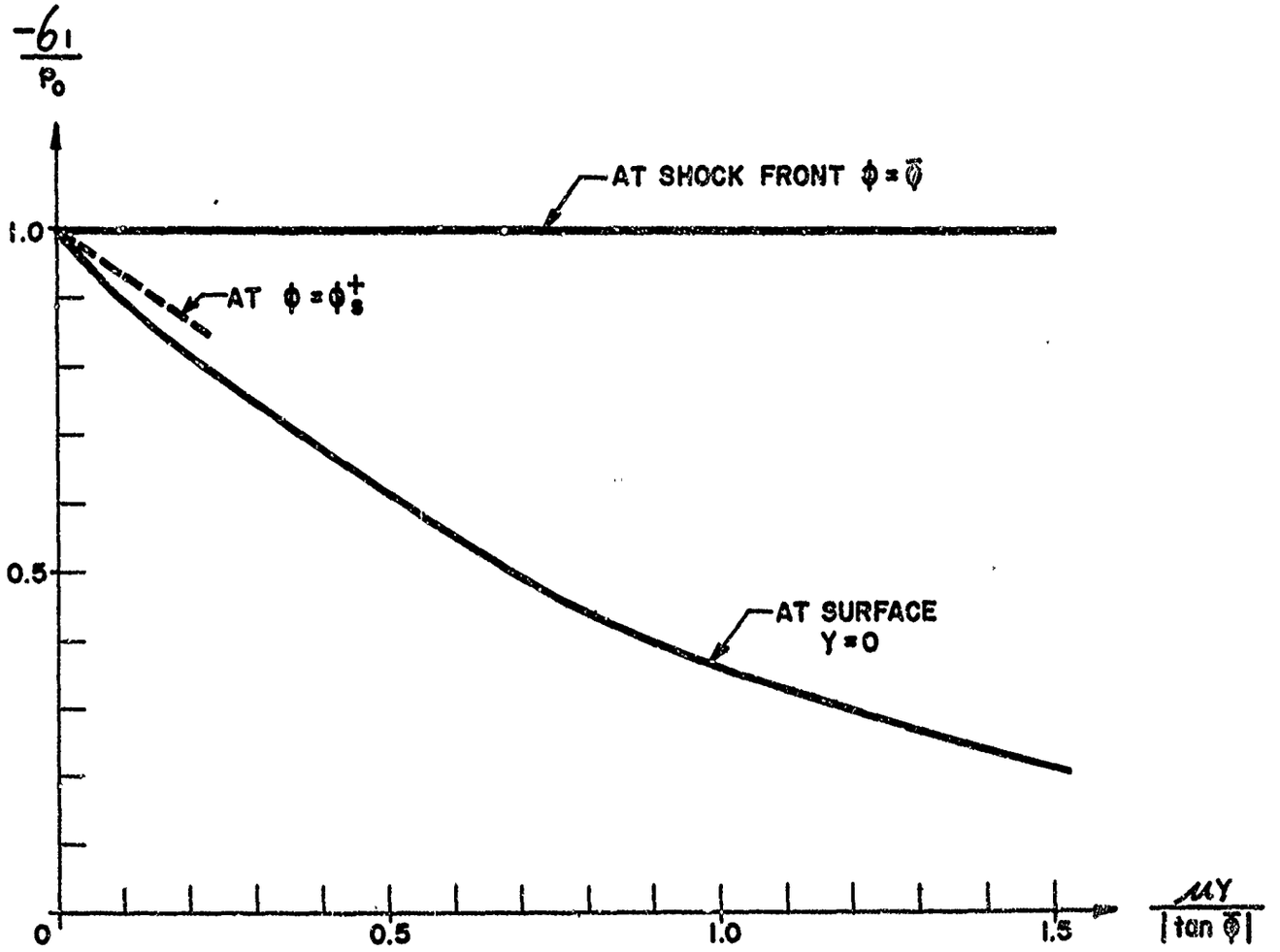

FIG. 17 PRINCIPAL STRESS σ_1 FOR
$\nu = 0.25$, $\alpha = 0.20$, $V/c_p = 5.0$

TABLE X

Results for $\nu = 0.333$, $\alpha = 0.10$, $V/c_p = 2.0$

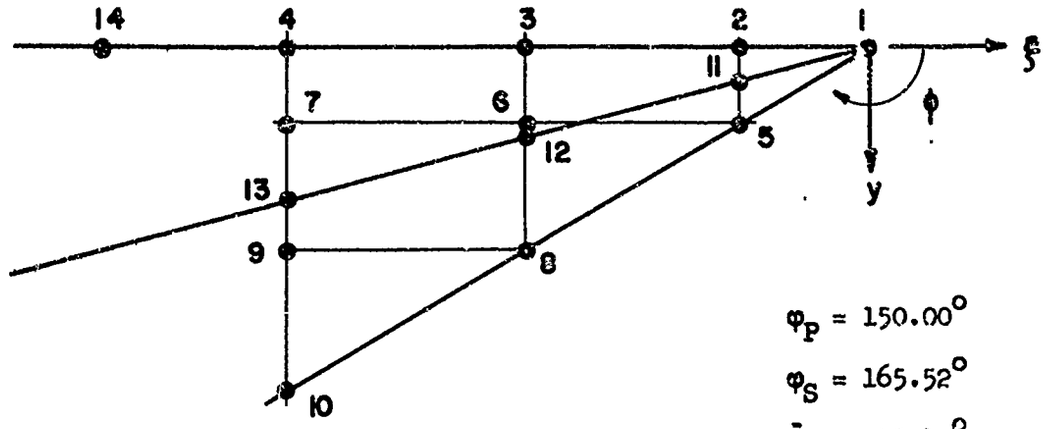

$\varphi_P = 150.00^\circ$

$\varphi_S = 165.52^\circ$

$\tilde{\varphi} = 150.42^\circ$

Point	$-\mu\xi$	μy	$-\sigma_1/p_o$	$-\sigma_2/p_o$	$-\sigma_3/p_o$	θ°	n
1 *	0	0	1.002	0.6155	0.6155	60.42	1.00
1 **	0	0	1.000	0.6179	0.6155	90.00	0.991
2	0.264	0	0.7678	0.4998	0.4987	90.00	0.878
3	0.705	0	0.4941	0.3605	0.3611	90.00	0.633
4	1.057	0	0.3458	0.2849	0.2865	90.00	0.378
5	0.264	0.15	0.9978	0.6127	0.6127	60.42	1.00
6	0.705	0.15	0.6797	0.3957	0.4343	100.8	1.02
7	1.057	0.15	0.4788	0.3089	0.3385	102.8	0.306
8	0.705	0.40	0.9902	0.6081	0.6081	60.42	1.00
9	1.057	0.40	0.6953	0.4602	0.4605	60.65	0.839
10	1.057	0.60	0.9842	0.6044	0.6044	60.42	1.00
11***	0.264	0.068	0.8827	0.5298	0.5469	94.79	1.02
12***	0.705	0.182	0.7310	0.3992	0.4526	102.4	1.13
13***	1.057	0.273	0.6403	0.3086	0.3919	107.6	1.29
14	1.30	0	0.2669	0.2447	0.2468	90.00	0.161

* Values at $\tilde{\varphi} \leq \varphi < \varphi_S$ ** Values at $\varphi_S < \varphi \leq \pi$

*** Values at $\varphi = \varphi_S^+$. At $\varphi = \varphi_S$, $\Delta\tau = +0.392\ p_o$.

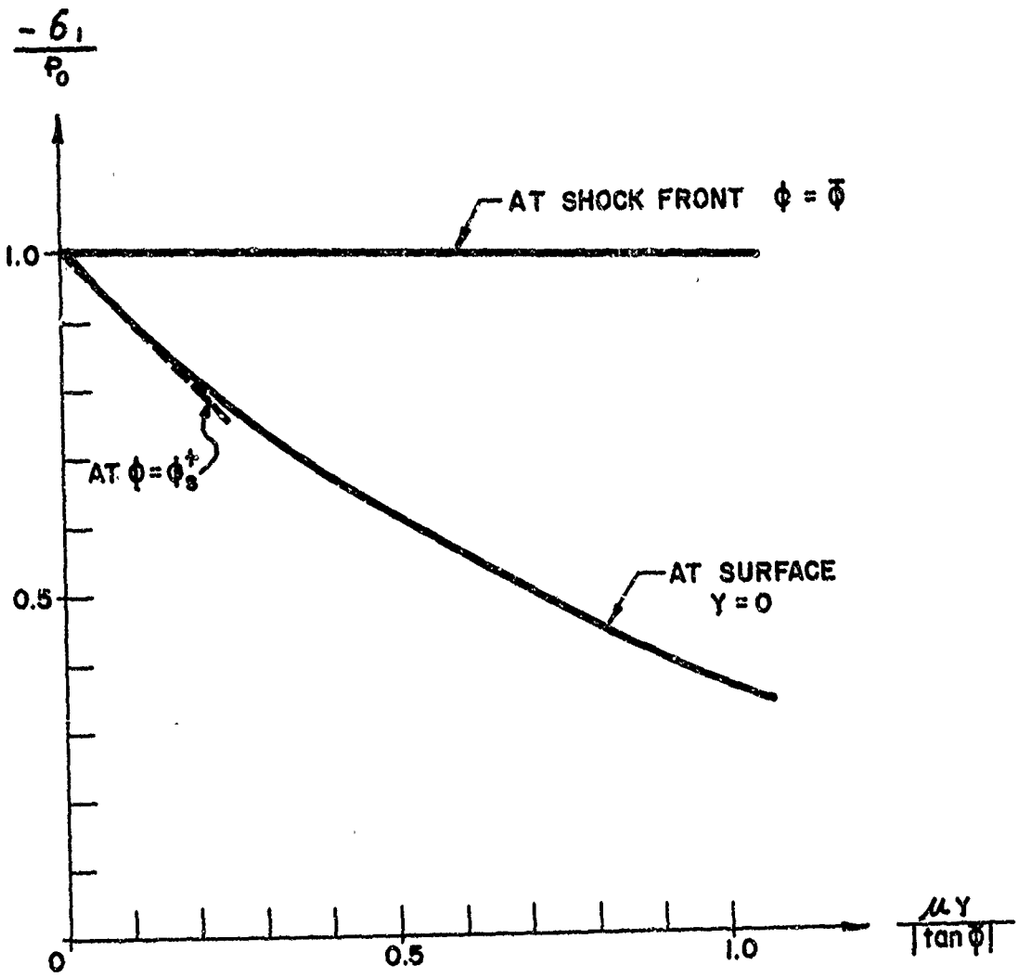

FIG. 18 PRINCIPAL STRESS σ_1 FOR
$\bar{V} = 0.3333$, $\alpha = 0.10$, $V/c_p = 2.0$

TABLE XI

Results for $\nu = 0.333$, $\alpha = 0.10$, $V/c_p = 5.0$

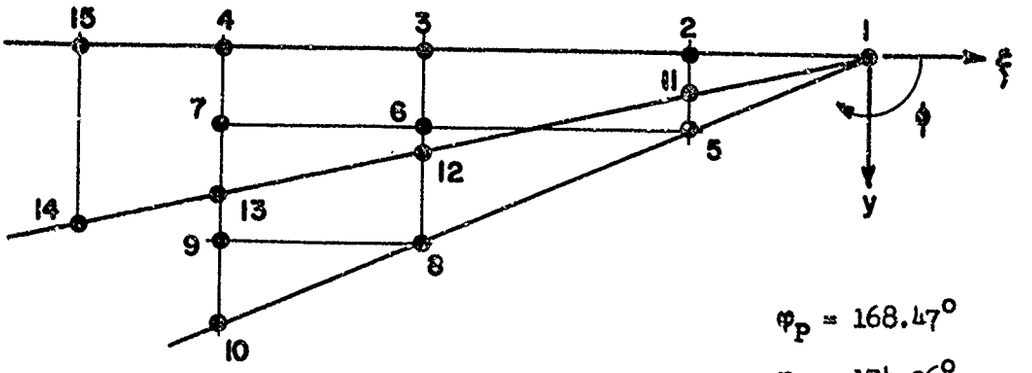

$\varphi_P = 168.47^\circ$

$\varphi_S = 174.26^\circ$

$\bar{\varphi} = 168.61^\circ$

Point	$-\mu\xi$	μy	$-\sigma_1/p_o$	$-\sigma_2/p_o$	$-\sigma_3/p_o$	θ°	n
1 *	0	0	0.9999	0.6140	0.6140	78.61	1.00
1 **	0	0	1.000	0.6139	0.6140	90.00	1.00
2	0.248	0	0.7802	0.5038	0.5040	90.00	0.892
3	0.745	0	0.4746	0.3507	0.3512	90.00	0.607
4	1.241	0	0.2847	0.2555	0.2561	90.00	0.210
5	0.248	0.05	0.9965	0.6119	0.6119	78.61	1.00
6	0.745	0.05	0.6112	0.4118	0.4168	94.68	0.790
7	1.241	0.05	0.3711	0.2937	0.2074	97.20	0.454
8	0.745	0.15	0.9897	0.6078	0.6078	78.61	1.00
9	1.241	0.15	0.6025	0.4134	0.4139	78.31	0.762
10	1.241	0.25	0.9830	0.6037	0.6037	78.61	1.00
11***	0.248	0.025	0.8841	0.5517	0.5545	91.93	0.960
12***	0.745	0.075	0.6946	0.4460	0.4559	96.88	0.882
13***	1.241	0.125	0.5515	0.3593	0.3790	103.5	0.820
14***	1.489	0.15	0.4945	0.3212	0.3472	107.4	0.804
15	1.489	0	0.2195	0.2130	0.2202	90.00	0.061

* Values at $\bar{\varphi} \leq \varphi < \varphi_S$ ** Values at $\varphi_S < \varphi \leq \pi$

*** Values at $\varphi = \varphi_S^+$ At $\varphi = \varphi_S$, $\Delta\tau = + 0.161\ p_o$.

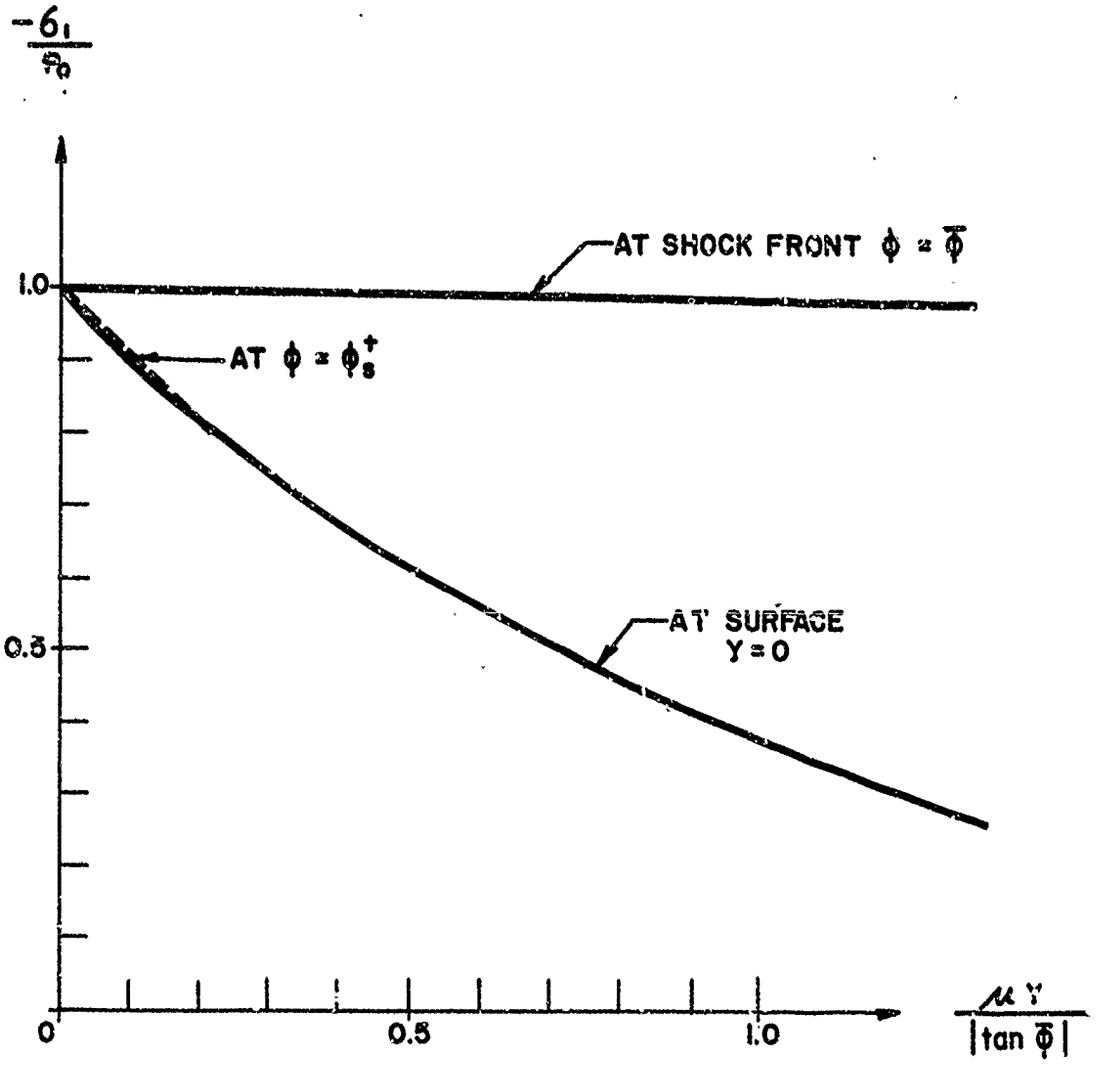

FIG. 19 PRINCIPAL STRESS σ_1 FOR
$\nu = 0.3333$, $\alpha = 0.10$, $V/c_p = 5.0$

TABLE XII

Results for $\nu = 0.05$, $\alpha = 0.05$, $V/c_p = 2.0$

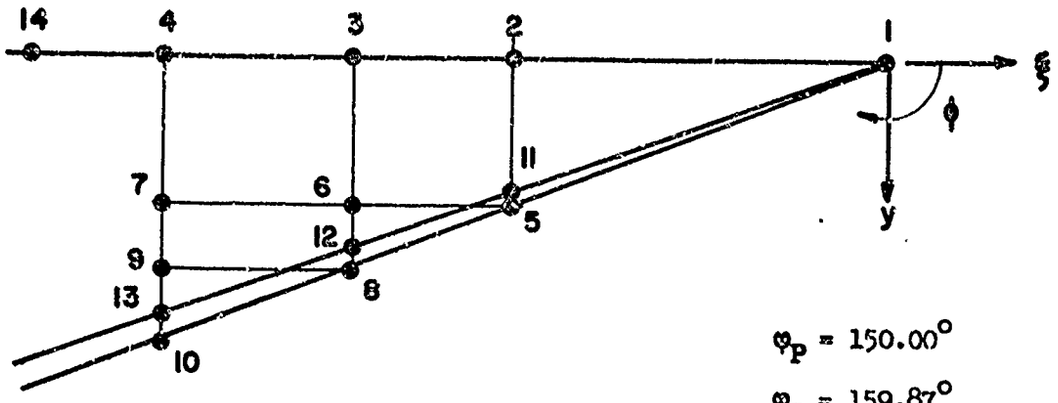

$\varphi_P = 150.00^\circ$

$\varphi_S = 159.87^\circ$

$\bar{\varphi} = 159.33^\circ$

Point	$-\mu\xi$	μy	$-\sigma_1/p_o$	$-\sigma_2/p_o$	$-\sigma_3/p_o$	θ°	n
1 *	0	0	0.9668	0.7527	0.7527	69.33	1.00
1 **	0	0	1.000	0.7195	0.7527	90.00	1.24
2	0.133	0	0.8759	0.7119	0.7461	90.00	0.741
3	0.398	0	0.6953	0.6719	0.7351	90.00	0.304
4	0.663	0	0.6775	0.5154	0.7264	90.00	1.151
5	0.133	0.05	0.9338	0.7270	0.7270	69.33	1.00
6	0.398	0.05	0.7420	0.6810	0.7151	88.79	0.286
7	0.663	0.05	0.6668	0.5687	0.7058	92.22	0.728
8	0.398	0.15	0.8721	0.6790	0.6790	69.33	1.00
9	0.663	0.15	0.6952	0.6381	0.6681	86.44	0.286
10	0.663	0.25	0.8156	0.6350	0.6350	69.33	1.00
11***	0.133	0.049	0.9640	0.6937	0.7275	90.43	1.24
12***	0.398	0.146	0.8989	0.6453	0.6804	91.30	1.24
13***	0.663	0.243	0.8396	0.6011	0.6372	92.15	1.24
14	0.795	0	0.6683	0.4512	0.7227	90.00	1.56

* Values at $\bar{\varphi} \leq \varphi < \varphi_S$ ** Values at $\varphi_S < \varphi \leq \pi$

*** Values at $\varphi = \varphi_S^+$. At $\varphi = \varphi_S$, $\Delta\tau = + 0.556\ p_o$.

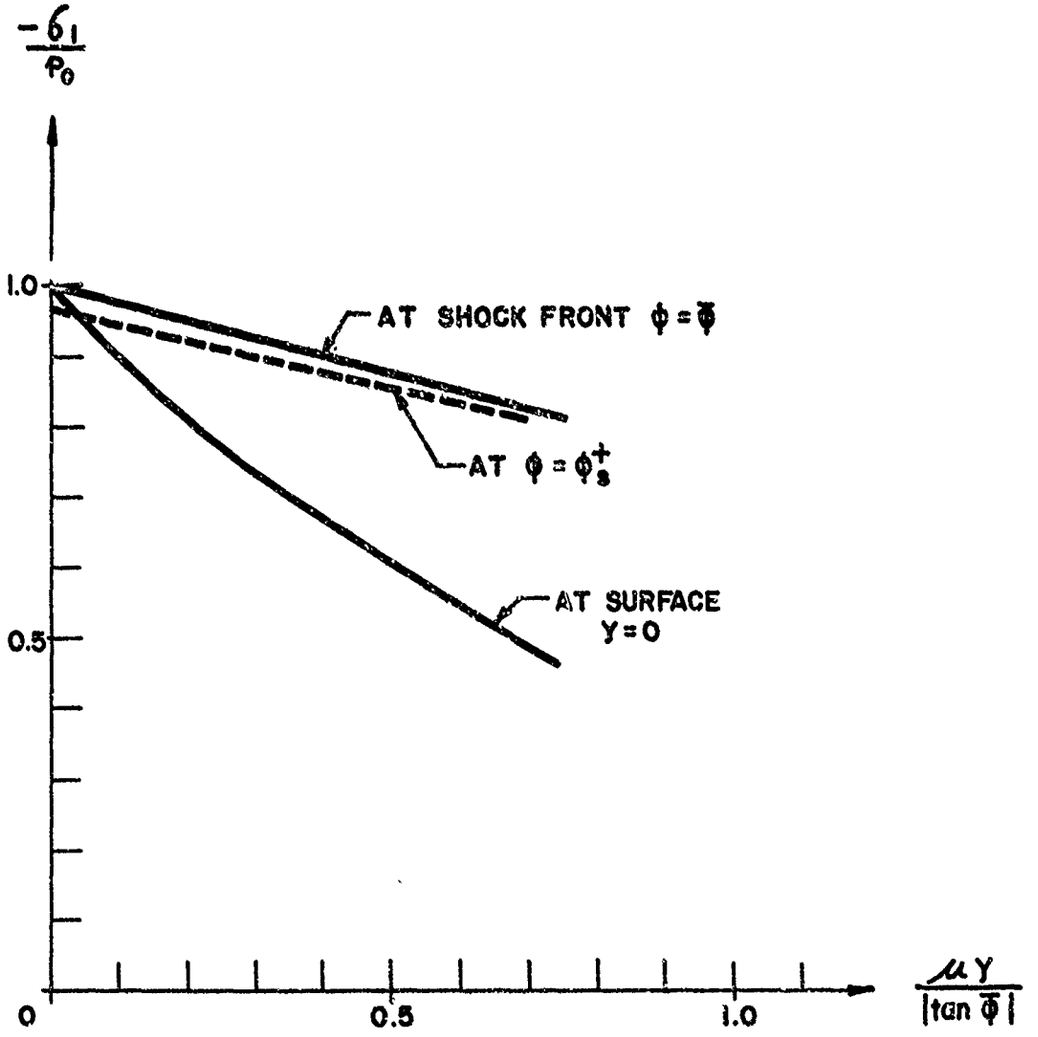

FIG. 20 PRINCIPAL STRESS σ_1 FOR
$\bar{v} = 0.05$, $\alpha = 0.05$, $V/c_p = 2.0$

that the largest violations $n > 1$ occur at points on the S-front. For the values of $\mu\xi$ considered above the violations are not greater than at point 1. The results for these three values of $\mu\xi$ may therefore be accepted as being in a region of good approximation. This desirable situation does, however, not continue for larger values of $(-\mu\xi)$. Points 13 and 14, both, show rapid increases in n indicating poor approximations for $|\mu\xi| > 1.30$. In the case discussed, the violations on the S-front are more severe than on the surface. This is typical for $V/c_p = 2$. For much larger values of this parameter, e.g., $V/c_p = 5$, Table III, it is seen that the violations on the surface $y = 0$ control the range of validity of the results.

Having established that the solution in the range of the variables ξ and y covered in Table II is a reasonably good approximation, the (approximate) solution found for the decaying pressure pulse can be compared with the (exact) solution [1] for the step wave to assess the importance of the decay. For the step pulse the peak stress $(-\sigma_1)$ at each target point occurs at the arrival of the S-front, the peak value remaining at $\sigma_1/p_o = -1$ for all depths. Figure 10 shows the decrease of the principal stress σ_1 with depth for the decaying pulse. It is seen that $(-\sigma_1/p_o)$ in the range shown decreases only to about 75%. It is important that this very moderate decrease is not just due to the fact that the solution applies only very close to the front of the applied load. This is demonstrated by Figure 10, which shows also the surface pressure that occurs at the point with the same abscissa ξ as the target point, and at the time of arrival of the plastic front at the target. This surface pressure decreases in the same range to about 25% of its original peak value. (It is noted that the decrease of peak pressure with depth for the decaying pulse is most pronounced for small values of α and ν, and that the example selected shows a faster decrease of the peak pressure with depth than all but one of the other cases listed in Tables III to XI. The exception is

the nonrepresentative case shown in Table XII.)

Figure 10 also shows the decrease of the peak pressure with depth due to the decaying pulse for an elastic material having the same value of Poisson's ratio ν. There is a slight decrease between $y = 0$ and $\mu y \simeq 0.055$, but for larger values of y there is no further decrease. The maximum decrease is about 7%. The effect of the decay of the pulse for the elastic-plastic material, while quite modest is several times larger than for the elastic material.

2. Typical results for $V/c_p = 5$

Consider again the case $\nu = 0.125$, $\alpha = 0.10$, for which the results are listed in Table III and the accompanying Fig. 11. The major difference between the results for $V/c_p = 2$ and those for $V/c_p = 5$ is the much smaller violation, $n = 1.02$, near the origin for the latter, and the fact that there are no further violations at all on the S-front at any of the points considered. The validity is limited by the violation at point 15 on the surface. It is typical for this value of V/c_p that violations on the S-front do not control, but that violations on the surface or the truncation limit the validity of the solution.

It is useful to compare the results for $V/c_p = 5$ with a simpler analysis for the limiting case $V/c_p \to \infty$. To consider the limiting case, the definition $\xi = x - Vt$, Eq. (32), is introduced into the surface load given by Eq. (46) for $x < Vt$

$$\sigma_y = - p_o e^{\mu\xi} = - p_o e^{\mu(x - Vt)} \qquad (60)$$

Consider now the time history of the surface pressure at a point, say $x = 0$, for $V \to \infty$. In the limit μ must go to zero, $\mu \to 0$, in such a way that μV becomes the

inverse of the decay time of the pressure,

$$\mu V \to \frac{1}{t_o} \tag{81}$$

The surface pressure in the limiting case is then

$$\sigma_y = - p_o e^{- t/t_o} \tag{82}$$

$V \to \infty$ implies that the pressure is applied simultaneously at all points on the surface of the half-space, i.e., the problem becomes a simple case of one dimensional propagation of a plane wave. The case is treated in Appendix III using the same general approach as in Sections II and III. Using this formulation for $V/c_p \to \infty$, the decrease of the peak pressure with depth was computed for several values of ν and σ. The results for the peak pressure agree to two significant figures with those for $V/c_p = 5$, providing a check on the two dimensional analysis. The comparison of the two cases also proves that estimates for the magnitude of the difference between the effect of step and decaying pressures for values of $V/c_p \gtrsim 4$ may be based on one dimensional analysis.

3. Range of depth for which results apply

The previous discussions considered the validity of the results only with respect to a nondimensional depth μy. It is appropriate to consider a value μ of physical interest to find out for what actual depth y results have been obtained.

Let $t_o = 0.2$ sec., $V = 4000$ ft/sec., and Eq. (81) becomes

$$\frac{1}{\mu} = V t_o = 800 \text{ ft.} \tag{83}$$

Table II, representing a typical case for $V/c_p = 2$, contains information on the peak pressure up to about $\mu y = 0.6$ or to a depth of about 480 ft. A time history can be plotted from points 8 and 9 and from an interpolated point on the S-front between points 12 and 13 for $\mu y = 0.4$ or at a depth of 300 ft.

For $V/c_p = 5$, where results are shown in Table III, the equivalent results reach only a depth of about 160 ft. However, in this case the one dimensional analysis in Appendix III, valid for somewhat larger depth, can be used below the depth of 160 ft, or one can use relatively simple finite difference schemes to reach any depth.

SECTION V

CONCLUSIONS.

An analytical approach has been presented and numerical results have been obtained for the effect of a decaying pressure pulse moving with superseismic velocity $V \gtrsim 2\, c_p$ on the surface of a half-space of elastic-plastic material subject to the yield condition, (1). This yield condition applies to a material with internal friction of the Coulomb type. Due to simplifications in the analysis the results obtained are approximate, and restricted to target points of limited depth, as discussed at length in Section IV.

Information on the stress field for exponential decay of the applied load is contained in Tables 2-12 and in the accompanying Figs. (10)-(20). Comparing the effects of step loads given in [1] with the new results for decaying loads, it is found that in the latter case the peak and subsequent pressures decrease with depth, which is not the case for a step load. However, the decrease found at any depth y is only a fraction of the decrease of the applied pressure at the point on the surface directly above the target point, i.e., a distance equal to $(-\, y/\mathrm{tg}\, \bar{\varphi})$ behind the shock front. The decrease is therefore less important than one might expect.

It has also been found that for velocities $V \gtrsim 4\, c_p$ useful information for the two dimensional case of progressing surface pressures may be obtained, approximately, from one dimensional analysis, which is naturally much simpler. E.g., it is not too difficult to formulate a finite difference analysis treating the problem considered approximately in Appendix C allowing for the additional plastic regions ignored in the Appendix. The validity of results obtained in such a fashion would then not be subject to the depth limitations which restrict the results obtained here.

APPENDIX I - Special Case of the Step Load, m = 0

Although an approach analogous to that used for $m > 0$ may also be used for the special case of the step load, $m = 0$, it is simpler to take the solution found in Appendix D of Ref. [1] directly. As discussed in Section II the solution has an inelastic pressure front, but is otherwise entirely elastic.

The stresses in the region $\bar{\varphi} \leq \varphi < \varphi_s$ are

$$\sigma_1 = \Delta\sigma \tag{84}$$

$$\sigma_2 = \sigma_3 = R\Delta\sigma \tag{85}$$

where

$$\Delta\sigma = - p_o \frac{\cos 2\varphi_s}{(1 - R)\cos^2(\bar{\varphi} - \varphi_s) + (1 + R)\cos^2\varphi_s - 1} \tag{86}$$

$$R = \frac{1 - \alpha\sqrt{3}}{1 + 2\alpha\sqrt{3}} \tag{87}$$

and σ_1 , σ_2 , σ_3 are the principal stresses. The stresses in the region $\pi \leq \varphi < \varphi_s$ are

$$\sigma_1 = - p_o \tag{88}$$

$$\sigma_2 = p_o + (1 + R)\Delta\sigma \tag{89}$$

$$\sigma_3 = R\Delta\sigma \tag{90}$$

The invariants required to check the violation of the yield condition are

$$J_1 = (1 + 2R)\Delta\sigma \tag{91}$$

$$J_2 = p_o^2 + (1 + R)\, p_o\Delta\sigma + \left(\frac{1 + R + R^2}{3}\right)(\Delta\sigma)^2 \tag{92}$$

APPENDIX II - Special Case of the Linear Term, m = 1

The equations governing the response of the system to a linear surface loading are obtained from the general expressions derived in Section III by setting the index m = 1. The potentials are then

$$\left.\begin{aligned} \phi^{(1)} &= a_0 y^3 + a_1 \xi y^2 + a_2 \xi^2 y + a_3 \xi^3 \\ \bar{\psi}^{(1)} &= b_0 y^3 + b_1 \xi y^2 + b_2 \xi^2 y + b_3 \xi^3 \\ \bar{\bar{\psi}}^{(1)} &= c_0 y^3 + c_1 \xi y^2 + c_2 \xi^2 y + c_3 \xi^3 \end{aligned}\right\} \tag{93}$$

There are twelve unknown coefficients a_i , b_i , c_i , (i = 0 to 3), and Eqs. (71)-(79) written for m = 1 provide twelve equations for their solution

$$6(M_S^2 - 2)\, a_3 + 4c_2 = -\frac{p_o}{G}\mu \tag{94}$$

$$4a_2 - 6(M_S^2 - 2)\, c_3 = 0 \tag{95}$$

$$\tan^2\varphi_S\,(b_1 - c_1) + 2\tan\varphi_S\,(b_2 - c_2) + 3(b_3 - c_3) = 0 \tag{96}$$

$$\begin{aligned} &6N_1 a_3 + 2(N_1 \tan\bar{\varphi} + N_2)\, a_2 + 2N_2 \tan\bar{\varphi}\, a_1 + 6N_4 b_3 + \\ &+ 2(N_4 \tan\bar{\varphi} + N_3)\, b_2 + 2N_3 \tan\bar{\varphi}\, b_1 = 0 \end{aligned} \tag{97}$$

$$\begin{aligned} &6N_5 a_3 + 2(N_5 \tan\bar{\varphi} + N_6)\, a_2 + 2N_6 \tan\bar{\varphi}\, a_1 + 6N_8 b_3 + \\ &+ 2(N_8 \tan\bar{\varphi} + N_7)\, b_2 + 2N_7 \tan\bar{\varphi}\, b_1 = 0 \end{aligned} \tag{98}$$

$$\begin{aligned} &6N_9 a_3 + 2(N_9 \tan\bar{\varphi} + N_7)\, a_2 + 2N_7 \tan\bar{\varphi}\, a_1 + 6N_{10} b_3 + \\ &+ 2(N_{10} \tan\bar{\varphi} - N_6)\, b_2 - 2N_6 \tan\bar{\varphi}\, b_1 = 0 \end{aligned} \tag{99}$$

$$
\left.
\begin{aligned}
a_1 &= 3(M^2 - 1)\, a_3 \qquad & b_1 &= 3(M_S^2 - 1)\, b_3 \\
a_o &= \frac{(M^2 - 1)}{3}\, a_2 \qquad & b_o &= \frac{(M_S^2 - 1)}{3}\, b_2 \\
& & c_1 &= 3(M_S^2 - 1)\, c_3 \\
& & c_o &= \frac{(M_S^2 - 1)}{3}\, c_2
\end{aligned}
\right\} \qquad (100)
$$

Substituting Eqs. (100) into Eqs. (94) to (99) reduces the system to six equations on the six unknowns a_3 , a_2 , b_3 , b_2 , c_3 , c_2 . Equations (94) and (95) do not change, while Eqs. (96)-(99) become

$$6(b_3 - c_3) + 2 \tan \varphi_S\, (b_2 - c_2) = 0 \qquad (101)$$

$$[6N_1 + 6N_2 \tan \bar{\varphi}\, (M^2 - 1)]\, a_3 + 2[N_1 \tan \bar{\varphi} + N_2]\, a_2 +$$
$$+ [6N_4 + 6N_3 \tan \bar{\varphi}\, (M_S^2 - 1)]\, b_3 + 2[N_4 \tan \bar{\varphi} + N_3]\, b_2 = 0 \qquad (102)$$

$$[6N_5 + 6N_6 \tan \bar{\varphi}\, (M^2 - 1)]\, a_3 + 2[N_5 \tan \bar{\varphi} + N_6]\, a_2 +$$
$$+ [6N_8 + 6N_7 \tan \bar{\varphi}\, (M_S^2 - 1)]\, b_3 + 2[N_8 \tan \bar{\varphi} + N_7]\, b_2 = 0 \qquad (103)$$

$$[6N_9 + 6N_7 \tan \bar{\varphi}\, (M^2 - 1)]\, a_3 + 2[N_9 \tan \bar{\varphi} + N_7]\, a_2 +$$
$$+ [6N_{10} - 6N_6 \tan \bar{\varphi}\, (M_S^2 - 1)]\, b_3 + 2[N_{10} \tan \bar{\varphi} - N_6]\, b_2 = 0 \qquad (104)$$

APPENDIX III - The Limiting Case $V/c_p \to \infty$

As a limiting case for very large values of V/c_p one obtains the one dimensional problem, where the surface load is applied uniformly everywhere on the surface, and decays exponentially in time (see Fig. A-1).

The applicable relations between stress rates and strain rates are

$$\dot{\epsilon}_x = \dot{\epsilon}_z = \dot{\epsilon}_{xy} = 0 \tag{105}$$

$$\dot{\epsilon}_y = \frac{\partial \dot{v}}{\partial y} = \frac{(1+\nu)(1-2\nu)}{E\,(1-\nu)}\,\dot{\sigma}_y \tag{106}$$

Integration with respect to time gives

$$\frac{\partial v}{\partial y} = \frac{(1+\nu)(1-2\nu)}{E\,(1-\nu)}\,\sigma_y + f_4(y) \tag{107}$$

$$\sigma_z = \sigma_x = \frac{\nu}{1-\nu}\,\sigma_y + f_5(y) \tag{108}$$

where f_4 and f_5 are arbitrary functions. Finally, the equation of motion is

$$\frac{\partial \sigma_y}{\partial y} = \rho\,\frac{\partial \dot{v}}{\partial t} \tag{109}$$

The solution of these differential equations may be expressed in terms of a single potential Φ and of one arbitrary function $g_3(y)$:

$$v = \Phi_y + g_3(y) \tag{110}$$

$$\dot{v} = \dot{\Phi}_{yt} \tag{111}$$

$$\sigma_y = \frac{2G\,(1-\nu)}{1-2\nu}\,\dot{\Phi}_{yy} \tag{112}$$

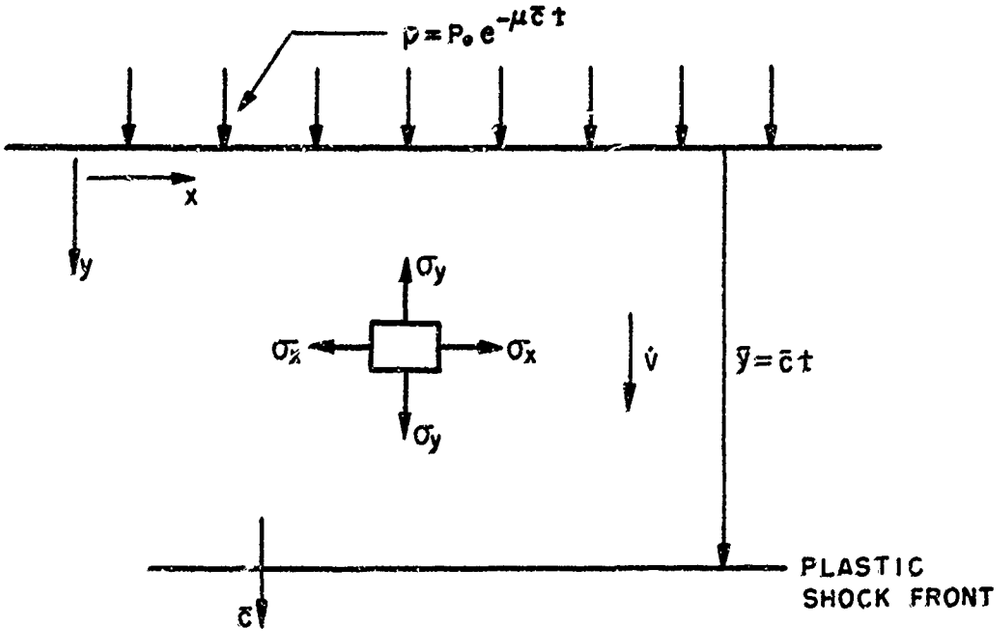
$p = P_o e^{-\mu \bar{c} t}$
x
y
σ_y
σ_x
σ_x
σ_y
$\dot{v}$
$\bar{y} = \bar{c} t$
$\bar{c}$
PLASTIC
SHOCK FRONT

FIG. A-1

where the potential ϕ satisfies the wave equation,

$$\phi_{yy} = \frac{1}{c_p^2}\phi_{tt} \tag{113}$$

and the functions $f_4(y)$ and $g_3(y)$ are related

$$f_4(y) = \frac{dg_3(y)}{dy} \tag{114}$$

The boundary conditions are

<u>at y = 0</u>

$$\sigma_y = -p_o e^{-\mu\bar{c}t} = -p_o \sum_{m=0}^{\infty} \frac{(-\mu\bar{c}t)^m}{m!} \tag{115}$$

<u>at y = $\bar{c}t$</u>

$$\sigma_y = -\rho\bar{c}\dot{v} \tag{116}$$

$$\sigma_x = \frac{1 - \alpha\sqrt{3}}{1 + 2\alpha\sqrt{3}}\sigma_y \tag{117}$$

The Taylor series expansions for ϕ has the form

$$\phi = \sum_{m=0}^{\infty} \phi^{(m)} \qquad \phi^{(m)} = \sum_{i=0}^{m+2} a_i^{(m)} (\bar{c}t)^i y^{m+2-i} \tag{118}$$

with m + 3 unknowns a_i .

Substituting this series into Eqs. (115)-(117) in the manner discussed in Section III yields m + 3 equations

$$a_{i+2} = \frac{c_p^2}{\bar{c}^2} \frac{(m + 2 - i)(m + 1 - i)}{(i + 2)(i + 1)} a_i \qquad i = 0 \text{ to } m \tag{119}$$

$$a_m = -\frac{(-1)^m}{m!} \frac{1-2\nu}{4(1-\nu)} \tag{120}$$

$$\frac{c_p^2}{c_2^2}(m+2)(m+1)\,a_0 + (m+1)\,a_{m+1} + \sum_{i=1}^{m}(m+2-i)\left[\frac{c_p^2}{c_2^2}(m+1-i)+i\right]a_i = 0 \tag{121}$$

The resulting values of a_i permit computation of the stresses σ_y and σ_z from Eqs. (112) and (108), respectively, where the function $f_5(y)$ is determined by Eq. (117).

DISTRIBUTION

No. cys	
	HEADQUARTERS USAF
	Hq USAF, Wash, DC 20330
1	(AFCOA)
1	(AFOCE)
1	(AFRSTG)
1	(AFIAC/TD-3, Capt Herman)
1	USAF Dep, The Inspector General (AFIDI), Norton AFB, Calif 92409
1	USAF Directorate of Nuclear Safety (AFINS), Kirtland AFB, NM 87117
	MAJOR AIR COMMANDS
	AFSC, Andrews AFB, Wash, DC 20331
1	(SCT, for RTTW)
1	(SCTR)
1	(SCTN)
1	TAC (DEE), Langley AFB, Va 23365
1	AUL, Maxwell AFB, Ala 36112
1	USAFA (DFLBA), Colo 80840
	AFSC ORGANIZATIONS
1	AFSC Scientific and Technical Liaison Office, Research and Technology Division, AFUPO, Los Angeles, Calif 90045
1	AF Materials Laboratory, Wright-Patterson AFB, Ohio 45433
1	ORA (RRRD), Holloman AFB, NM 88330
1	ESD (ESTI), L. G. Hanscom Fld, Bedford, Mass 01731
1	SAMSO (BSR), AFUPO, Los Angeles, Calif 90045
1	APGC (PGBPS-12), Eglin AFB, Fla 32542
1	RADC (EMLAL-1), Griffiss AFB, NY 13442
	KIRTLAND AFB ORGANIZATIONS
	AFSWC, Kirtland AFB, NM 87117
1	(SWEH)
1	(SWT)
	AFWL, Kirtland AFB, NM 87117
11	(WLIL)
30	(WLDC)
1	(WLRP)
2	(WLRT)

DISTRIBUTION (cont'd)

No. cys

OTHER AIR FORCE AGENCIES

Director, USAF Project RAND, via: AFLO, The RAND Corporation, 1700 Main Street, Santa Monica, Calif 90406

1 (Dr. H. Brode)

1 (Dr. C. C. Mow)

1 (RAND Library)

1 AFOSR, 1400 Wilson Blvd, Arlington, Va 22209

1 AFCRL, L. G. Hanscom Fld, Bedford, Mass 01731

ARMY ACTIVITIES

1 Chief of Research and Development, Department of the Army (CRD/P, Scientific and Technical Information Division), Wash, DC 20310

1 US Army Materiel Command, NIKE-X Field Office (AMCPM-NXE-FB, Lt Col F. G. Thomas), Bell Telephone Laboratories, Inc., Whippany, NJ 07981

1 Commanding Officer, Ballistic Research Laboratories (AMXBR-TB, Mr. J. Meszaros), Aberdeen Proving Ground, Md 21005

1 Commanding Officer, US Army Electronics Research and Defelopment Laboratory, Ft Monmouth, NJ 07703

1 Commanding Officer, US Army Research Office-Durham, Box CM, Duke Station, Durham, NC 27706

1 Chief of Engineers (ENGMC-EM), Department of the Army, Wash, DC 20315

2 Director, Army Research Office, 3045 Columbia Pike, Arlington, Va 22204

Director, US Army Waterways Experiment Sta, P. O. Box 631, Vicksburg, Miss 39181

5 (WESRL)

1 (Mr. Donad Day)

1 (Mr. Guy Jackson)

2 Director, US Army Engineer Research and Development Laboratories, ATTN: STINFO Branch, Ft Belvoir, Va 20260

1 Commanding General, White Sands Missile Range (Tech Lib), White Sands, NM 88002

1 Commandant, US Army Ordnance School, Aberdeen Proving Ground, Md 21005

2 US Army Engineer Division, Ohio River, Corps of Engineers (ORDLBVR), 5851 Mariemont Avenue, Mariemont, Cincinnati, Ohio 45227

NAVY ACTIVITIES

1 Chief of Naval Research, Department of the Navy, Wash, DC 20390

1 Naval Air Systems Command (RRRU), Department of the Navy, Wash, DC 20360

UNCLASSIFIED

Security Classification

DOCUMENT CONTROL DATA - R&D

(Security classification of title, body of abstract and indexing annotation must be entered when the overall report is classified)

1. ORIGINATING ACTIVITY *(Corporate author)*
Paul Weidlinger, Consulting Engineer
New York, New York 10017

2a. REPORT SECURITY CLASSIFICATION
UNCLASSIFIED

2b. GROUP

3. REPORT TITLE
EXPONENTIALLY DECAYING PRESSURE PULSE MOVING WITH SUPERSEISMIC VELOCITY ON THE SURFACE OF A HALF SPACE OF GRANULAR MATERIAL

4. DESCRIPTIVE NOTES *(Type of report and inclusive dates)*
May 1966-May 1967

5. AUTHOR(S) *(Last name, first name, initial)*
Bleich, Hans H.; Matthews, Alva

6. REPORT DATE	7a. TOTAL NO. OF PAGES	7b. NO. OF REFS
July 1967	80	2

8a. CONTRACT OR GRANT NO.	AF 29(601)-7082	9a. ORIGINATOR'S REPORT NUMBER(S)
b. PROJECT NO.	5710	AFWL-TR-67-21
c. Subtask No.	13.144	9b. OTHER REPORT NO(S) *(Any other numbers that may be assigned this report)*
d.		

10. AVAILABILITY/LIMITATION NOTICES This document is subject to special export controls and each transmittal to foreign governments or foreign nationals may be made only with prior approval of AFWL (WLDC), Kirtland AFB, NM, 87117. Distribution is limited because of the technology discussed in the report.

11. SUPPLEMENTARY NOTES	12. SPONSORING MILITARY ACTIVITY
(Distribution Limitation Statement No. 2)	AFWL (WLDC) Kirtland AFB, NM 87117

13. ABSTRACT

An approximate solution is given for the effect of an exponentially decaying pressure pulse traveling with superseismic velocity on the surface of a half space. The material of the half space is an elastic-plastic model of a material having internal Coulomb friction. The yield condition selected may be suitable for a granular material. The effect of a step wave for this geometry and medium was treated previously. For that case, the peak pressures do not decrease with increase in depth, while such a decrease is obtained for a decaying surface load. It was the prime purpose of this investigation to determine the magnitude of this attenuation. The approximate solutions obtained are valid for a limited distance behind the wave front, and are tabulated for 11 different sets of parameters pertaining to the material and velocity. The tabulated results show that the peak pressures in the case of the decaying surface load do decrease with depth, but that the decrease is less than one might intuitively expect.

DD FORM 1 JAN 64 1473

UNCLASSIFIED

Security Classification

UNCLASSIFIED

Security Classification

14. KEY WORDS	LINK A		LINK B		LINK C	
	ROLE	WT	ROLE	WT	ROLE	WT
Elastic-plastic Wave propagation Ground motion Granular media						

INSTRUCTIONS

1. ORIGINATING ACTIVITY: Enter the name and address of the contractor, subcontractor, grantee, Department of Defense activity or other organization *(corporate author)* issuing the report.

2a. REPORT SECURITY CLASSIFICATION: Enter the overall security classification of the report. Indicate whether "Restricted Data" is included. Marking is to be in accordance with appropriate security regulations.

2b. GROUP: Automatic downgrading is specified in DoD Directive 5200.10 and Armed Forces Industrial Manual. Enter the group number. Also, when applicable, show that optional markings have been used for Group 3 and Group 4 as authorized.

3. REPORT TITLE: Enter the complete report title in all capital letters. Titles in all cases should be unclassified. If a meaningful title cannot be selected without classification, show title classification in all capitals in parenthesis immediately following the title.

4. DESCRIPTIVE NOTES: If appropriate, enter the type of report, e.g., interim, progress, summary, annual, or final. Give the inclusive dates when a specific reporting period is covered.

5. AUTHOR(S): Enter the name(s) of author(s) as shown on or in the report. Enter last name, first name, middle initial. If military, show rank and branch of service. The name of the principal author is an absolute minimum requirement.

6. REPORT DATE: Enter the date of the report as day, month, year; or month, year. If more than one date appears on the report, use date of publication.

7a. TOTAL NUMBER OF PAGES: The total page count should follow normal pagination procedures, i.e., enter the number of pages containing information.

7b. NUMBER OF REFERENCES: Enter the total number of references cited in the report.

8a. CONTRACT OR GRANT NUMBER: If appropriate, enter the applicable number of the contract or grant under which the report was written.

8b, 8c, & 8d. PROJECT NUMBER: Enter the appropriate military department identification, such as project number, subproject number, system numbers, task number, etc.

9a. ORIGINATOR'S REPORT NUMBER(S): Enter the official report number by which the document will be identified and controlled by the originating activity. This number must be unique to this report.

9b. OTHER REPORT NUMBER(S): If the report has been assigned any other report numbers *(either by the originator or by the sponsor)*, also enter this number(s).

10. AVAILABILITY/LIMITATION NOTICES: Enter any limitations on further dissemination of the report, other than those imposed by security classification, using standard statements such as:

(1) "Qualified requesters may obtain copies of this report from DDC."

(2) "Foreign announcement and dissemination of this report by DDC is not authorized."

(3) "U. S. Government agencies may obtain copies of this report directly from DDC. Other qualified DDC users shall request through _____."

(4) "U. S. military agencies may obtain copies of this report directly from DDC. Other qualified users shall request through _____."

(5) "All distribution of this report is controlled. Qualified DDC users shall request through _____."

If the report has been furnished to the Office of Technical Services, Department of Commerce, for sale to the public, indicate this fact and enter the price, if known.

11. SUPPLEMENTARY NOTES: Use for additional explanatory notes.

12. SPONSORING MILITARY ACTIVITY: Enter the name of the departmental project office or laboratory sponsoring *(paying for)* the research and development. Include address.

13. ABSTRACT: Enter an abstract giving a brief and factual summary of the document indicative of the report, even though it may also appear elsewhere in the body of the technical report. If additional space is required, a continuation sheet shall be attached.

It is highly desirable that the abstract of classified reports be unclassified. Each paragraph of the abstract shall end with an indication of the military security classification of the information in the paragraph, represented as *(TS), (S), (C), or (U)*.

There is no limitation on the length of the abstract. However, the suggested length is from 150 to 225 words.

14. KEY WORDS: Key words are technically meaningful terms or short phrases that characterize a report and may be used as index entries for cataloging the report. Key words must be selected so that no security classification is required. Identifiers, such as equipment model designation, trade name, military project code name, geographic location, may be used as key words but will be followed by an indication of technical context. The assignment of links, rules, and weights is optional.